COSMIC RAY GROUP

School of Physics and Astronomy

FACILITY FORM 602

N70-12550 (ACCESSION NUMBER)

(THRU) 1

42 (PAGES)

(CODE)

CR#107162 (NASA CR OR TMX OR AD NUMBER)

29 (CATEGORY)

UNIVERSITY OF MINNESOTA

Electron Precipitation Patterns and Their Relation to Substorm Increases In 50-150 keV Electrons at the Synchronous Orbit*

by

Lowell H. Rosen

Cosmic Ray Technical Report No.

CR-145

August, 1969

School of Physics and Astronomy
University of Minnesota
Minneapolis, Minnesota

* A thesis submitted to the University of Minnesota Graduate School in partial fulfillment for the requirement for the degree of Master of Science.

Abstract

Analysis of records from the seven station Alaskan Riometer Chain (L = 3.9 to L = 8.) shows that the median latitude location of the hard (above 40 keV) electron precipitation region extends from a low latitude edge (defined as maximum intensity/e) of L = 5 for all local times to a high latitude edge of beyond L = 8 during the morning and to between L = 6 or 7 during the afternoon. With the aid of the riometer chain, the poleward and equatorward progression in precipitation onset was studied. The poleward progression events were most frequently seen near local midnight, and on the average, the time lag for the events showing the equatorward progression increased with local time between midnight and noon. Comparisons of the electron precipitation events at the riometer chain with increases of electron fluxes at the ATS-1 synchronous orbit show that a good correlation in coincidence, intensity and latitude exists. The events used in this analysis indicate the source of much of substorm precipitation between 0400 and 1200 local time is an eastward drifting, dribbling electron cloud. However, for some substorms, acceleration occurring at all local times is not ruled out.

I. Introduction

Akasofu (1964) has shown that auroral activity is centered around local midnight and usually exhibits a cyclic morphology lasting from one to three hours which is commonly termed an auroral substorm. Simultaneous with the occurrence of the auroral substorm is an increase in activity of the earth's magnetic field shown by bay-type changes in the horizontal component of the surface field measured near the polar regions (polar magnetic substorms). Although much of the visible auroral activity is centered about local midnight and extends from dusk to dawn, there appears to be a larger scale world-wide phenomena taking place which has been termed magnetospheric substorm by Parks (1968b) and others (Jelly and Brice, 1967). Occurring with the auroral and polar magnetic substorms are increases in radiation belt electron fluxes (above 50 keV) and electron precipitation at all local times (Parks and Winckler, 1968). The substorm correlated energetic electrons appear to be accelerated from lower energy particles during the substorms. The location and nature of the acceleration is still not well known. Also, the nature of the relation of substorm precipitation to the energetic (above 50 keV) electron increases in the radiation belts is not well understood.

Parks et al. (1968) showed that there was a very good correlation between electron flux (50-150 keV) increases at the geostationary ATS-1 satellite and precipitation near the ATS-1 field line. The electron precipitation was measured indirectly by monitoring with a balloon-borne scintillation counter the bremsstrahlung X-rays produced when the precipitated electrons collide with the molecules of the atmosphere.

This correlation will be further examined with the aid of the seven station Alaskan Riometer Chain and the ATS-1 satellite. Although the absorption measurement by riometers cannot be as precisely converted back to a precipitated electron flux as can X-ray measurements, the riometer chain has merit since it can simultaneously monitor a much larger region of precipitation. Small scale features of the precipitation are averaged out (space-time averaging) and the large scale features (such as peak absorption, onset, pulsations, etc.) of the electron precipitation can then be compared to electron increases at the synchronous orbit. Since the riometer chain stations are located along the magnetic meridian passing through College, Alaska, it is also suited for determining the latitude extent of the substorm precipitation region and for examining the north-south progression of the precipitation onset which was seen by Jelly and Brice (1967) and others. Determining the behavior of these large scale features of electron precipitation as a function of local time and their correlation to electron increases (50-150 keV) at the ATS-1 will be helpful in solving the substorm acceleration and precipitation problem. This will be the principal objective of this paper.

II. Data Sources

Electron fluxes in the radiation belts were measured with the aid of the University of Minnesota electron spectrometer aboard the ATS-1 satellite. The ATS-1 is in a geostationary orbit and thus lies in the equatorial plane at a distance of 6.6 earth radii from the center of the earth. The spectrometer measures electron fluxes in the energy ranges of 50-150 keV, 150-500 keV and 500-1000 keV. The detector window is normally located with respect to the field lines so that only trapped electrons with pitch angles between 60° and 90° are sampled (Lezniak et al., 1968).

Electron precipitation near the ATS-1 field line was monitored with the Alaskan Riometer Chain. The Alaskan Riometer Chain consists of seven riometers operating simultaneously at 30 MHz and lying along the magnetic meridian passing through College, Alaska. The stations have L values of 3.9, 4.2, 4.5, 5.0, 5.5, 6.3 and 8. Their locations together with the location of the base of the ATS field line are shown on the map in Figure 1. The chain is operated by the Space Disturbance Laboratory of ESSA. Herbert H. Sauer and George Reid of ESSA have made the data available for this study.

III. Data Analysis.

Riometers measure precipitation in terms of absorption of the radio frequency cosmic noise background according to the definition, Absorption = 10 $\mathrm{Log}_{10}(I_o/I)$ in units of decibels. "I" is the transmitted cosmic noise measured during precipitation, and "I_o" is the undisturbed background level, which has seasonal and diurnal variation. A precipitation measurement in terms of absorption is convenient since, for a given spectrum of precipitating electrons, the amount of absorption is roughly proportional to $(\mathrm{flux})^{1/2}$ of the ionizing precipitation (for riometer theory, see Little and Leinbach, (1958) and Ansari, (1964)). Also, the amount of absorption at a particular frequency is a function of the ionospheric condition and not of the riometer used. All the riometer records shown in this paper have I plotted on a linear scale. Absorption is indicated by an excursion of I below the background line, I_o.

In this analysis, absorption events are defined as periods of increased absorption lasting from 1/2 hour to 3 hours which reach a peak absorption of at least 1/3 db. During very disturbed times it sometimes becomes difficult to decide if a stretch of absorption is one event or a series of events. This situation, however, arises infrequently as compared to the total number of events. In addition, this decision has little consequence on the results of this analysis.

All the statistical studies presented in this paper were made on events occurring between March 18, 1967 and May 27, 1967. This interval was selected because good quality simultaneous data exists for the riometers and ATS-1 much of the time. To reduce biasing, all events within this time interval were used, providing the data quality was acceptable and events met all the specified requirements.

IV. Results.

A. Correlation of Electron Preipitation and Electron Flux (50-150 keV) Increases at the ATS-1 Orbit during Magnetospheric Substorms.

A sample of the correlation between ATS-1 measured electron increases and precipitation near the ATS-1 field line is shown in Figure 2. The simultaneous data for March 19, 1967 shows a series of substorm increases (identified with AE index) at the ATS, which have a semi-periodic nature and last from one to three hours. Accompanying all of the larger (above 10^6 electrons $cm^{-2}sec^{-1}ster^{-1}$) ATS electron increases is riometer absorption (absorption is in the downward direction). The March 19 sample period suggests that a one to one correspondence between the ATS-1 measured electron increases and electron precipitation may exist during substorms. To check this hypothesis, a large number of events was examined. The events were selected from the periods between March 18, 1967 and May 27, 1967, for which simultaneous data was available. These periods are March 18-20, March 23-27, April 1-3, April 6-10, April 13-17 and April 19-21. In order to show that the correspondence is indeed one to one, ATS electron increase events must be selected and checked for accompanying precipitation. Also, precipitation events must be selected and checked for accompanying electron increases at the ATS.

ATS-1 electron increases of about substorm period (1-3 hours), whose maximum intensity was at least a factor of 1.3 larger than the intensity at the beginning of the increase, were selected. Anything smaller than this becomes difficult to recognize. Ninety-two events were found in this interval which satisfied the criteria. Next, a search was made on the riometer records between L = 5.5 and L = 8. for accompanying precipitation coincident to at least 15 minutes. A scatterplot in Figure 3 shows the correlation between the ATS-1 electron increases and the precipitation increases. The symbols slightly to the left of the vertical axis are ATS-1 events for which no precipitation was found. The symbols offset slightly to the right of the vertical axis are ATS-1 events for which only a trace of precipitation was found. Although for these cases the precipitation could be detected, it was still too small to measure accurately because their intensities were less than .2 db. The remainder of symbols represent cases where a measurable precipitation was found. The symbols correspond to the local time sectors where the events were observed. A legend is given at the top of the graph.

Several things are evident from this plot. There appears to be a size correlation existing between the peak ATS increases and the peak precipitation increases at L = 6.3 which is dependent on local time (the "Δ's" define a line of less slope than the "$\times$'s" do). The 15% of the ATS increases that showed no accompanying precipitation were all small. This lack of correlation in 15% of the cases may exist because the precipitation is also small and is below the threshold sensitivity of the riometer. Thus, at least 85% of the observed increases of electrons at the ATS-1 are accompanied by precipitation coincident to 15 minutes.

Next, we will determine how often precipitation at the riometer chain is accompanied by 50-150 keV electron increases at the ATS orbit. This is slightly more difficult to do since the base of the ATS field line moves about and the exact position is not known. However, if we impose the criteria that the precipitation must occur simultaneously between L = 5.5 and L = 8., chances are good that the ATS field line will pass near that region. Of the 26 precipitation events which satisfy this criteria, 24 or 92% were accompanied by an increase at the ATS. The two exceptions (March 27, 1967 0410-0500 and April 21, 1967 0900-1100) could possibly represent cases where the magnetosphere was extremely distorted so that the ATS-1 field line did not pass through the precipitation region examined.

Twelve simultaneous riometer chain and ATS-1 events are shown in Figures 6 to 18. ATS-1 one minute averages were plotted along with tracings of the original riometer records (noise spikes removed). Most events show good correlation for features larger than ten minutes and often for features smaller than this. The events were not selected because of their good correlation, but rather because they represent a typical correlation for events of this size range. In terms of onset time, time of maximum and of fine features, the L = 5.5 and L = 6.3 riometers correlate best with electron increases at the ATS-1. The measurement of auroral type precipitation by riometers is too crude to warrant a more mathematical study of the correlation that was given above.

A random sample study of 25 increase events shows that over 90% are accompanied by marked increases in the AE index. Thus, the one to one correspondence between electron flux (50-150 keV) increases at the ATS-1 and electron precipitation near the ATS-1 field line occurring during magnetospheric substorms appears to be well established. Nearly all (92%)

of the precipitation events (greater than 1/3 db peak absorption) had ATS-1 increases accompanying them. The ATS-1 increases were more often accompanied by precipitation in the combined dawn and noon sectors (91%) than in the combined evening and midnight sectors (76%). This may result from the fact that the ATS-1 electron events were less intense during the evening and midnight hours and the precipitation intensity may have been below the sensitivity threshold of the riometer in some cases. The local time dependence of the size correlation will be discussed after the remainder of the results of this study are presented.

B. Latitude Extent of the Precipitation Regions.

With the aid of the seven station riometer chain, a more accurate determination of the extent in magnetic latitude of individual precipitation events can be made for all local times than was before possible. It is convenient to use the McIlwain L parameter as a measure of the magnetic latitude. During individual events, the shape of a distribution (as a function of L) of the peak absorptions measured with the seven riometers usually resembles a Gaussian closely enough so that the value of L where the peak absorption decreases to 1/e of the maximum can be determined. Defining this as the edge of the precipitation region rather than using the value of L for which absorption is no longer detectable reduces the effects which riometer sensitivity would have upon comparison of events of different intensities.

When constructing a distribution from only seven points, some approximations must be made. One difficulty is not knowing what the maximum of the distribution is since it may actually lie between two points. The largest of the peak absorptions will be chosen as the maximum of the distribution. For this approximation to be good, the maximum must not lie at one of the two end points. This requirement was met for almost all the events analyzed. The seven points were connected with straight lines and the value of L, for which the absorption drops to 1/3 of the maximum, was found from this.

Over 80 events were analyzed in this fashion and each is represented on the graph in Figure 4 as a vertical line segment. The end points of the line segment are the value of L where the maximum/e condition exists. If this point lay outside L = 3.9 to L = 8., an arrow was plotted instead. The events were plotted at the local time at which the measurement was made. The time used was that at the middle of the event.

The events have been grouped into two hour local time intervals. Within each interval, the median extent of both the upper and lower edge of the precipitation region was found. It is represented on the graph as a horizontal time segment. The median instead of the average extension was used since this better represents a typical event. Also, this enables one to find a representative number even though only a lower limit to the edge of the precipitation region is known for some of the events. For several of the two hour intervals, only a lower limit to the upper edge of the precipitation was known for a majority of the events. Thus, only a lower limit of the median extension could be found. No horizontal line segment is drawn for these cases.

The median of the lower edge of the precipitation region seems quite well fixed between L = 4.6 and L = 5.1. However, the median of the upper edge pulls in from beyond L = 8 during the morning hours to L = 6 or 7 during the afternoon and early evening.

C. North-South Progression of Precipitation Onset.

When examining simultaneous records from the stations of the riometer chain, it is observed that the absorption does not always begin simultaneously at all stations, but instead, the onsets progress either northward or southward along the chain. Its appearance resembles that which could be caused by the bulk motion of the precipitation region toward or away from the magnetic pole, although this need not be the explanation. A good example is shown in Figure 14. There is a progression toward low L values of both the onset and the maximum of the event. To determine better the significance of this feature of substorm precipitation, a study was done on a large number of events occurring at various local times. Events were chosen which had absorption of at least 1/3 db on at least three adjacent riometers.

There is quite a large degree of variability in absorption events and for this reason it becomes difficult to compare accurately the different events without using a large number of parameters. However, when using a large number of parameters, the physical significance of the phenomenon becomes more difficult to realize. For this study then, the progression will be represented with just one parameter. Since the progressive lag often appears at at least three successive stations, a decision must be made as to which pair to measure the lag between. Stations were chosen which showed the sharpest onset features and which best represented the trend occurring. Since the lags were not always measured between the same pair of riometers, the lags had to be normalized before different events could be compared. To do this, some assumption had to be made on the relation of the lag to L. For purposes to become apparent later, the relationship lag = $T_1 - T_2$ = const $\left(\frac{1}{L_1} - \frac{1}{L_2} \right)$ will be used. $T_1 - T_2$ is the onset time of the smaller L riometer minus the onset of the larger L riometer. Using this, the projected time lag between L = 3.9 and L = 8. can be found. This projected lag will then be the single parameter by which events can be compared. Since this method is somewhat artificial, the results must be interpreted with caution and in the light of the assumption made.

A total of 121 events met the established criteria and have been plotted vs. the local time (Figure 5) of the start of the event. A positive lag means that the high L riometer detected the absorption first, while a negative lag means the lower L riometer detected the absorption first. A lag equal to zero means the absorption starts simultaneously within error at all the affected riometers. The error in projected lag is about ± 15 minutes for all events. The horizontal bars represent the averaged projected lag during a two hour interval of local time. Between the hours of 0 and 12 UT, there is a trend for the average projected lag to increase steadily with local time. During these hours, the local time latitude distribution shown in Figure 4 remains fairly constant. In any case, one can see that the trend cannot be artificially induced through the assumed normalizing equation. Also, the grouping of negative lags (northward progression) near the midnight hour is a real effect and cannot be induced by the methods of this analysis.

V. Discussion

A. Discussion of Results.

Studies by Hartz and Brice (1967) show that electron precipitation during substorms is hard (above 40 keV) near the latitude location of the Alaskan Riometer Chain for all local times except those near midnight. The softer precipitation (about 10 keV) normally is seen at higher magnetic latitudes (above 70°) Near midnight, both hard and soft precipitation is observed at the riometer chain latitudes. The highest latitude, L = 8, riometer may sometimes lie in the region of the softer precipitation. As a whole, however, the riometer chain probably is measuring precipitated electrons near the energy range of the electrons measured by ATS-1 (50-150 keV). This is also suggested by the frequently good correlation between electron increases measured at the ATS-1 and riometer absorption.

Since, for a given flux of precipitated particles, the amount of absorption measured with riometers is strongly dependent upon the energy spectrum of the precipitated particles and on the local ionospheric conditions, it is not worthwhile to determine the extent of the correlation of absorption with the ATS-1 measured flux increases to a greater degree than was done in this analysis. Within the limitations of riometers, it was found that the electron flux (50-150 keV) increases at the synchronous orbit correlated in size and coincidence with precipitation near the nominal position of the ATS-1 field line. A simplified picture that emerges from these results is that of a cloud of energetic trapped electrons connected via the earth's magnetic field lines to the precipitation regions. The size, intensity and location of the cloud reflects the size, intensity and location of the precipitation region. Thus, precipitation appears to be intimately related to the conjugate increases in the trapped electrons.

The extent in L of the cloud of trapped electrons is probably similar to the extent in L of the precipitation region. If this is the case, it is interesting to note that the location of the energetic electron cloud lies in the region of the plasma sheet (about 1 keV electrons) as reported by Vasylunias (1968). The inner edges of the two regions coincide quite closely.

In Section IV-A we showed that there is a local time effect on the size correlation between electron increases at the ATS-1 and absorption at L - 6.3 (Ft. Yukon). For a given absorption, the accompanying ATS-1 increase near noon is smaller than the accompanying increase near dawn. This may be due to the fact that the ATS-1 orbit is normally outside the L = 6.3 field line. Then, depending on the separation in L between the ATS-1 and the L = 6.3 field line and upon the sharpness of the distribution in L of the electron intensities in the cloud, the electron flux at the ATS-1 will be some fraction less than the flux at the L = 6.3 field line. Near local noon, the magnetosphere is compressed due to interactions with the solar wind. Because of this compression, the ATS-1 is farther separated from the L = 6.3 field line at noon than it is at dawn. Also, as one can see from Figure 4, the distribution in L is sharper after local noon. These two local time dependent variations could couple to produce the observed local time effect upon the correlation of the ATS-1 increases with the absorption at L = 6.3.

Because of the orientation of the riometer chain, it is difficult to separate out the time variations in precipitation from the variations in absorption which are due to a longitudinal motion of the entire precipitation region. This separation is necessary before a complete solution to the substorm acceleration and precipitation problem can be found. The difficulty can be in part overcome by using the results of the studies by Hargreaves (1967) and Jelly and Brice (1967).

Hargreaves (1967) gave evidence for a bulk longitudinal motion of the precipitation region. He found that the substorm precipitation originates near midnight and moves longitudinally in both the eastward and westward directions. Measurements on a large number of events showed that precipitation regions observed during the local times of 0000 and 1400 have average eastward motion. Between the local times of 1400 and 2400, events displaying the eastward motion and events displaying the westward motion were both seen. The average motion during this local time is westward. The velocity of motion of the precipitation regions is near that of the gradient drift of a 40 keV electron with little or no electric fields present. This drift is in the eastward direction and thus could account for only the eastward moving precipitation regions. Jelly and Brice (1967) also observed this eastward motion and suggested that it may be produced by drifting electrons. The westward motions cannot be explained in terms of drift unless appropriate electric fields are added.

An example illustrating the bulk longitudinal motion is shown in Figure 18. Kiruna is located near midnight and the Alaskan Riometer Chain near local noon. Kiruna has about the same L value as College. The sudden onset and maximum of the precipitation at Kiruna clearly precedes that of the riometer chain. The electron flux (50-150 keV) increase at the ATS-1 correlated well with the absorption increase at the riometer chain as is usually the case. This means that a cloud of energetic electrons near the equatorial plane travels along with the eastward moving precipitation region and is connected to it by the earth's magnetic field lines.

The eastward motion of the cloud appears to be caused by a gradient drift of trapped particles. There are several observations which point to this. The field lines on the morning side within the ATS orbit are normally closed. This means that the electron increases observed at the ATS-1 are trapped electrons (pitch angles between 60° and 90°). In the absence of strong electric fields in the magnetosphere, the trapped electrons will drift at about the same angular velocity as the precipitation regions are observed to move.

Another observation which indicates that the motion of the cloud of trapped electrons may be a gradient drift is the lag observed in event onset for riometers on the same magnetic meridian but separated in latitude. The northernmost (high L) stations usually see the precipitation first for all local times except near midnight. This could be explained by the fact that the gradient drift period t is given by $t = \frac{44}{LE}$ where t is in minutes, L is the McIlwain parameter and E is the energy of the electrons in meV. Thus, electrons in the outer L shells drift around the earth faster than inner shell electrons of the same energy. The average observed lag should then be dependent on the local time where the observations are made.

One can see from Figure 5 that the precipitation events near midnight are not always simultaneous at all L values, but instead, are sometimes seen first at larger L values and sometimes first at smaller L values. If one considers these events near midnight as the distribution of initial orientations of the precipitation regions, it is clearly shown on the graph that the average normalized lag between the event onset at L = 3.9 and L = 8. increases during the hours of 0000 and 1200 local time. The theoretical prediction was calculated from the equation

$$t_{L=3.9} - t_{L=8.} = \frac{44}{E} \left(\frac{1}{3.9} - \frac{1}{8} \right)$$

for both E = 50 keV and E = 100 keV drifting electrons is also shown. The agreement for the hours between 0000 and 1200 is quite good for E = 50 keV.

Although the agreement is good, it should be viewed with some caution, because of the assumption made when normalizing the lags. Since the lags were not always measured between the same pair of riometers,they were all normalized to a lag between the riometer at L = 3.9 and the riometer at L = 8. Thus, some kind of relation between L shells and lag time had to be assumed. Since we wanted to show that the observed lag could be explained solely in terms of a differential drift, the observed lags were extrapolated to one between L = 3.9 and L = 8., by using the shape of the curves predicted by differential drift. This procedure should not induce a trend as prominent as the one seen between 0000 and 1200 local time nor should it significantly affect the slope.

Because of the qualitative nature of riometer measurements, this analysis of the north-south progression was somewhat subjective. Also, the possible spectral dependence of precipitation with L was ignored. Therefore, the results of the north-south progression study should be left open to controversy. However, since the north-south progression has been previously discussed (Jelly and Brice, 1967), an attempt to explain it is justified.

The median latitude extension of hard precipitation events as seen in Figure 2 is widest during the morning hours (0000-1200) and narrows during the afternoon hours. There are several possible explanations for this. One is that the boundary of the magnetosphere may be pushed in close enough to the earth near noon so that the eastward drifting electrons are blocked off. The narrowing of the precipitation zone may also be reflecting that a different type of precipitation event predominates before 1400 (eastward moving) than after 1400 (westward moving).

B. Dribbling Cloud Model of Electron Precipitation.

Thus far, the association of substorm precipitation with a drifting cloud of electrons has been discussed, but little has been said concerning the nature of their relationship. Although somewhat speculative, one can set up a model of substorm precipitation which is based on the results of this analysis and Hargreaves' observations. Hargreaves showed that the bulk of the precipitation is initially located near midnight, but the longitudinal size was not determined. It seems reasonable that the initial longitudinal location of the precipitation region is where most of the electrons are accelerated. It is also likely that some of the freshly accelerated electrons will be immediately precipitated because of their small pitch angles. Since the acceleration must last for a time on the order of an hour (period of a substorm), precipitation seen at the local time of the production region could be that resulting directly from the acceleration plus that dribbling from a drifting cloud of electrons which remained trapped after the acceleration. If the above model is correct, some idea of the size and location of the acceleration region can be inferred. The observation (top of Figure 19) is made that the median peak electron intensity at the ATS-1 during substorms is largest near 0400 local time. If the production region was narrow and located about midnight, the location of the maximum substorm intensities would be difficult to explain in terms of a dribbling drifting cloud alone, for which one might expect the precipitation to steadily decrease and not go through a maximum. One way to overcome this difficulty is to assume that the production region is fairly widespread in local time and extends eastward to around 0400 local time. Then, if the accelerated flux was fairly uniform over the entire production region, a maximum flux would be seen near 0400 local time since the contribution of drifting particles would be greatest at this location. It is not ruled out that some substorm acceleration takes place simultaneously at all local times. However, its contribution to the total particle flux near the equatorial plane and to precipitated fluxes must be small beyond 0400 local time since the observed lag between longitudinally separated riometers indicates that the source for a bulk of the precipitated particles is moving.

Figure 19 (top) shows that the median peak electron flux at the ATS-1 during substorms decreases during the hours of 0400 to 1700 local time. An exponential curve with a time constant of 8.3 local time hours has been fitted to the points for this local time interval. Assuming a drifting, dribbling cloud model of electron precipitation, one can determine if for this local time the rate of decrease in the number of electrons in the cloud is sufficient to account for the amount of precipitation observed. A rough calculation can be made by assuming that the flux at the ATS is isotropic and monoenergetic at 100 keV. Then, by Louisville's theorem, the total intensity (electrons-cm^{-2}-sec^{-1}) is the same anywhere along a field line. If the precipitated loss of electrons is slow enough so that the pitch angle distribution remains somewhat isotropic throughout redistribution, then by Louisville's theorem, the precipitated intensity is equal to the change in intensity at the ATS-1. The precipitated electron intensity can then be converted into absorption by using Ansari's (1964) calculations, which were for a 36 MHz riometer during midnight hours. The absorption varies with about the inverse square of the riometer operating frequency and the conversion factors were adjusted according to 30 MHz.

The amount of precipitation predicted from this dribbling cloud model is shown as the solid curve on Figure 19 (bottom). The median observed precipitation is shown as circles. Although the model prediction is slightly low, the agreement is quite reasonable in view of the rough calculation that was made. It is observed that the median substorm size decreases to 1/e of the maximum in about 8.3 hours of local time. For gradient drifting 50 keV particles this means that the tubes of flux would empty to 1/e in about 3×10^3 seconds. O'Brien (1962) calculated the lifetimes of greater than 45 keV trapped between 60° and 70° magnetic latitude to be 3×10^3 to 2×10^4 secs, which agrees quite well. Thus, it seems quite reasonable that a significant portion of the hard morning precipitation results from electrons drained out of a drifting cloud of previously accelerated electrons.

During the hours of 1400-2400 local time, Hargreaves (1967) observed both eastward and westward moving precipitation regions with the average motion being westward. The eastward motion seen at these local times is probably an extension of the eastward motion seen between 0000 and 1400 local time. The westward motion, however, cannot be explained in terms of drift unless electric fields are involved. One possible explanation of the westward motion could be westward surges described by Akasofu (1964). Their velocities of .17 to 1.7 km/sec are slightly small compared to the 3.7 km/sec velocity observed by Hargreaves.

The results in Figure 5 of the north-south progression vs. local time analysis show a deviation from that which would be predicted from differential drift after about local noon. After local noon, if the positive lag events were identified with the eastward moving regions and the zero lag events identified with westward moving regions and neglected, the remainder of the events would follow quite well for all local times the theoretical prediction for a time lag produced by different drift periods at different L shells.

VI. Summary

The median latitude extent of the hard (above 40 keV) precipitation was established as a function of local time. The lower latitude edge, defined by maximum intensity/e, is near L = 5 for all local times. The upper latitude edge is beyond L = 8. during the morning hours and pulls in to between L = 6 and 7 during the afternoon hours.

The poleward and equatorward progression in onset of precipitation was examined and is found to depend strongly on local time. The poleward progressions (- lag in Figure 3) are congregated in the midnight hours. The equatorward progression (+ lag) increases with a local time starting near midnight. This result is, however, still open to controversy because of the methods and subjective nature of the analysis.

This analysis also shows that a nearly one to one correspondence exists between flux increases of 50-150 keV electrons at the geostationary ATS-1 satellite and increases in electron precipitation near the ATS-1 field line. An intensity correlation also exists between the two. As one might expect, the ATS-1 electron increases correlate best with the L = 5.5 and L = 6.3 riometers.

The above correlation results together with the observation made most recently by Jelly and Brice and by Hargreaves of a bulk eastward motion of the precipitation regions indicate that the eastward moving precipitation regions are accompanied by a cloud of energetic electrons which then is also moving, due probably to gradient drift. Jelly and Brice, and Hargreaves suggested this, but had no direct evidence for the cloud. Since the gradient drift period is inversely proportional to L, the observation that the high L riometers, on the average, detect the precipitation first during the post midnight hours can be accounted for. It is also suggested that the narrowing of the precipitation zone after noon could result from the boundary of the magnetosphere being pushed in far enough near noon such that the eastward drifting particles in the high L shells are blocked off. The median substorm intensity of electrons measured at the ATS-1 decreases with local time after 0400. Assuming a drifting, dribbling cloud model, the rate of decrease is sufficient to account for the observed precipitated intensities between 0400 and 1200 local time.

Acknowledgments

The author is greatly indebted to Professor J. R. Winckler for his guidance and helpful discussions throughout the data analysis and writing of this thesis.

The author is also indebted to George K. Parks for his continued interest and numerous discussions over this work.

Thanks is given to Herbert Sauer and George Reid of ESSA for the use of the riometer chain data which made this analysis possible.

This study is supported by the National Aeronautics and Space Administration under contract no. NGL-24-005-008 and the National Science Foundation under contract no. GA-1508.

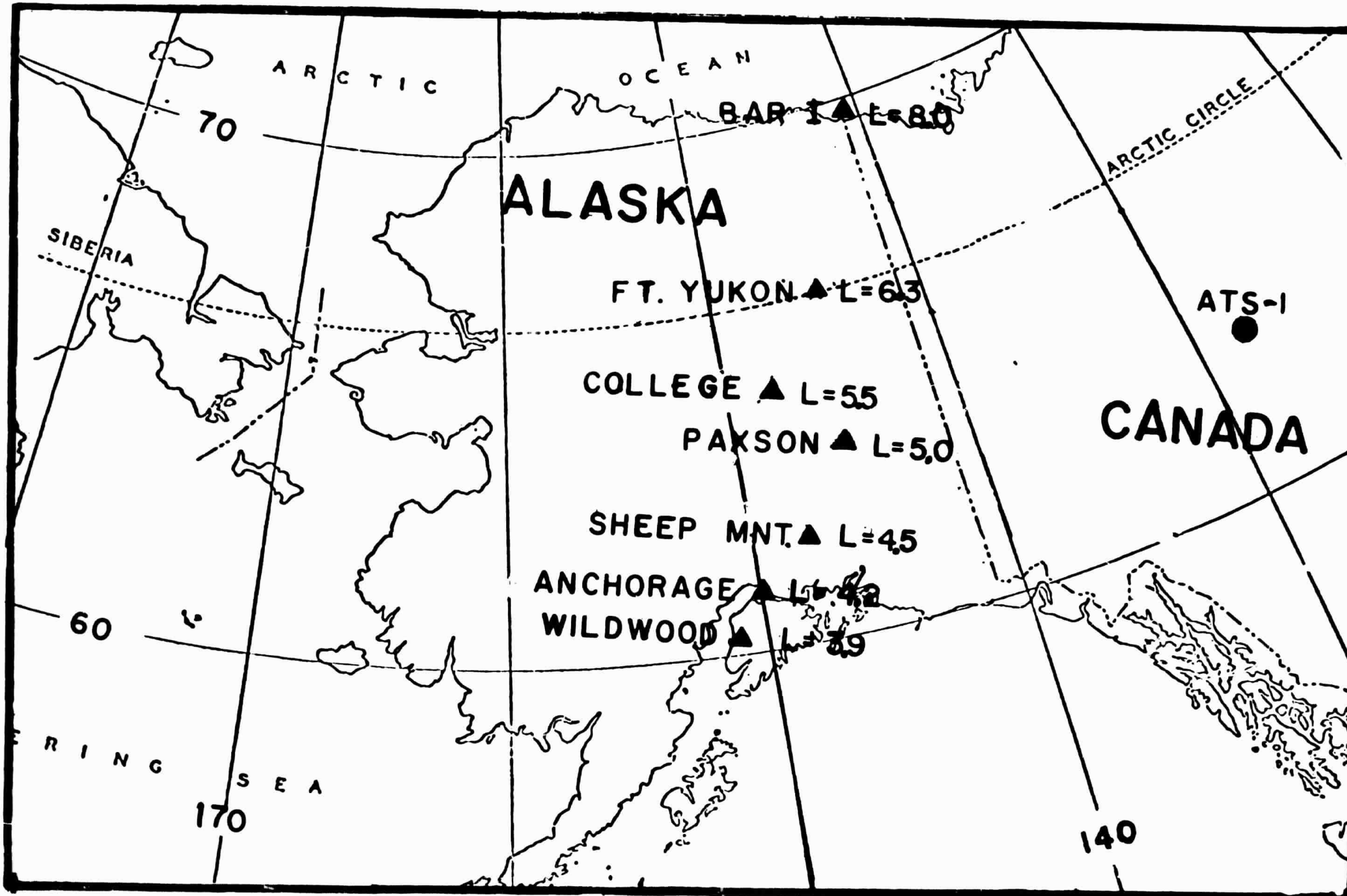

ALASKAN RIOMETER CHAIN

Fig. 1

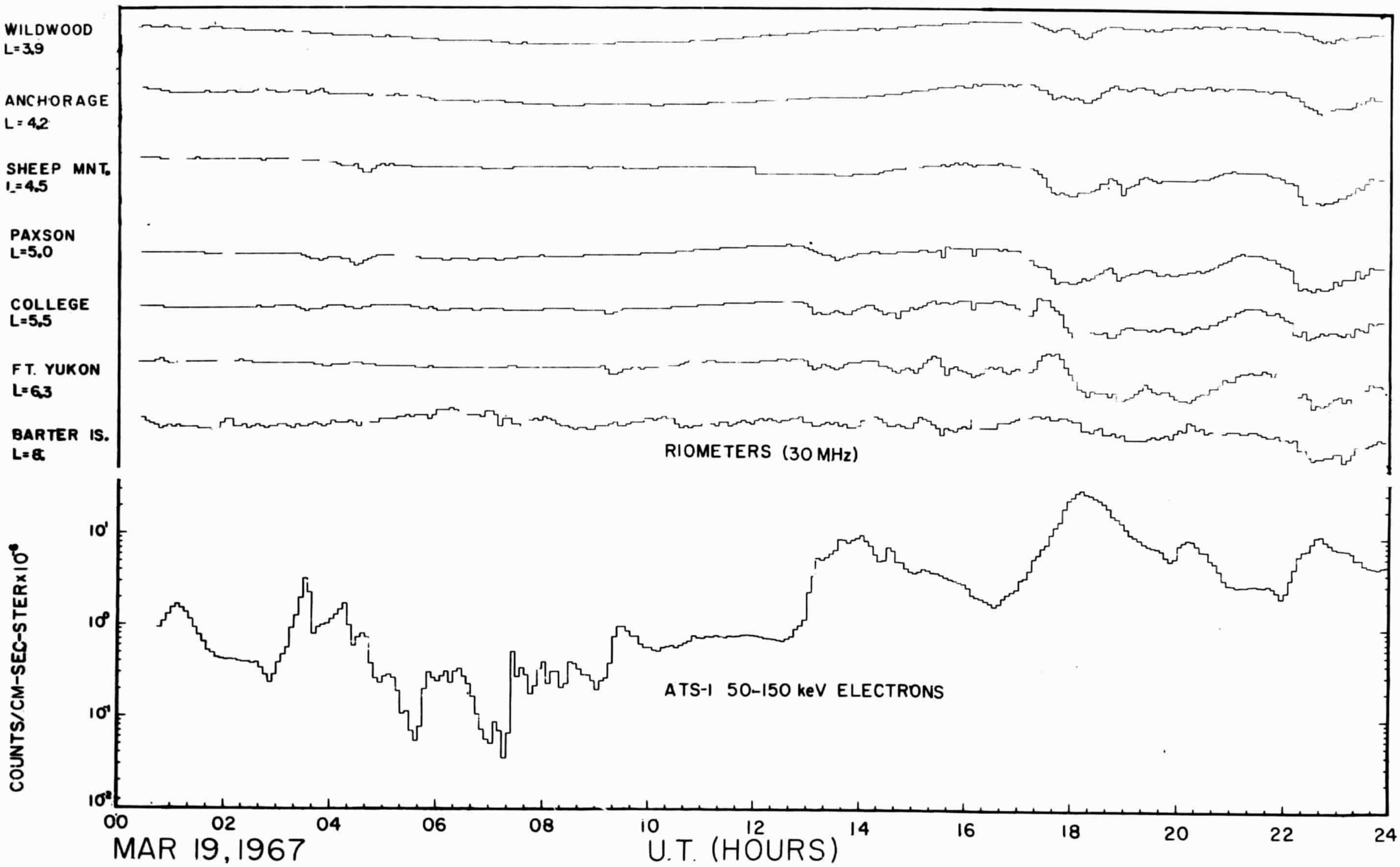
WILDWOOD L=3.9
ANCHORAGE L=4.2
SHEEP MNT. L=4.5
PAXSON L=5.0
COLLEGE L=5.5
FT. YUKON L=6.3
BARTER IS. L=8
RIOMETERS (30 MHz)
COUNTS/CM-SEC-STER×10^6
10^1
10^0
10^-1
10^-2
ATS-1 50-150 keV ELECTRONS
00
02
04
06
08
10
12
14
16
18
20
22
24
MAR 19, 1967
U.T. (HOURS)

Fig. 2

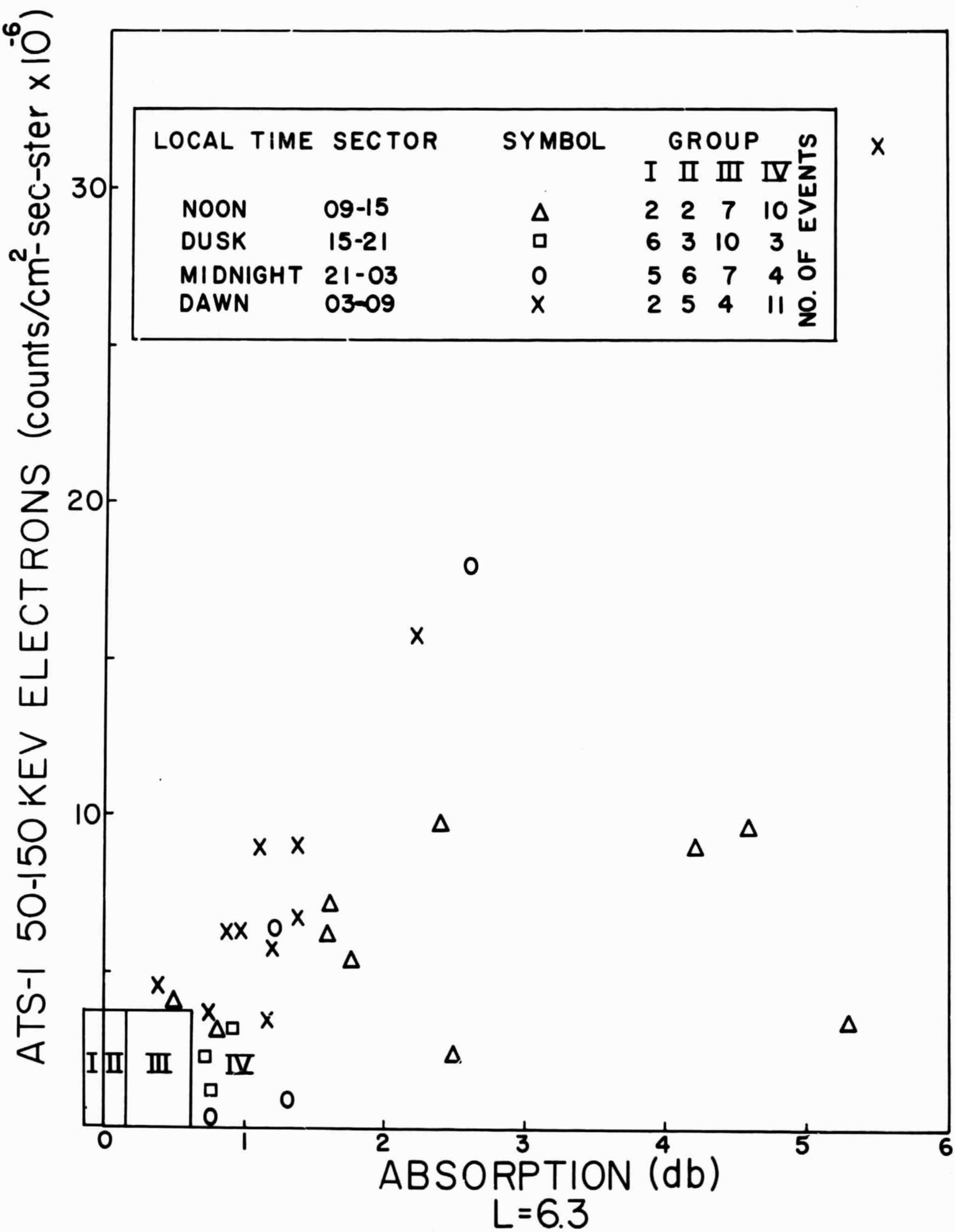

LOCAL TIME SECTOR
SYMBOL
GROUP
I II III IV
NO. OF EVENTS
NOON 09-15 Δ 2 2 7 10
DUSK 15-21 □ 6 3 10 3
MIDNIGHT 21-03 O 5 6 7 4
DAWN 03-09 X 2 5 4 11
ATS-1 50-150 KEV ELECTRONS (counts/cm²-sec-ster x 10⁻⁶)
ABSORPTION (db)
L=6.3
I
II
III
IV
0
1
2
3
4
5
6
10
20
30

Fig 3

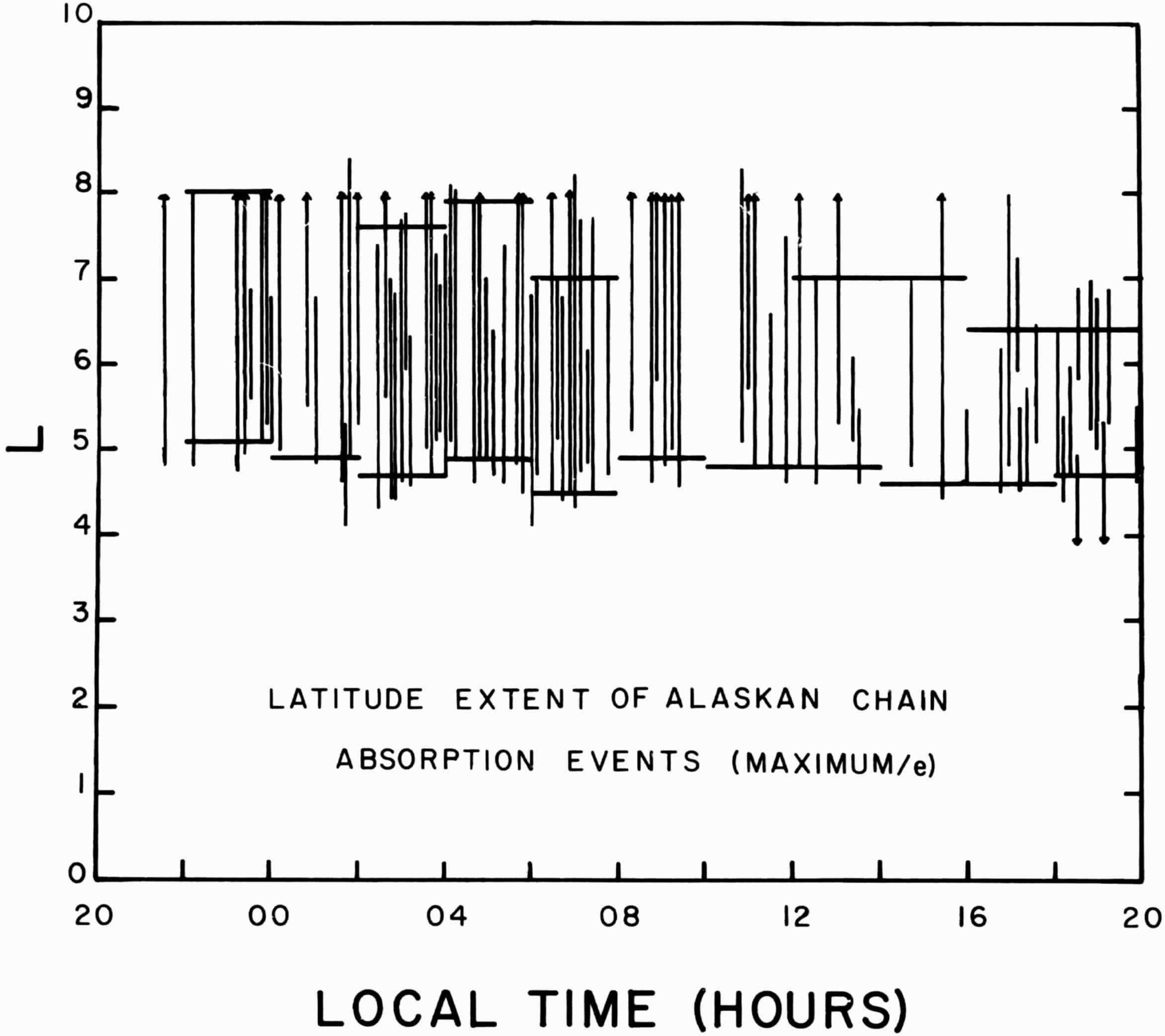

LATITUDE EXTENT OF ALASKAN CHAIN
ABSORPTION EVENTS (MAXIMUM/e)
L
10
9
8
7
6
5
4
3
2
1
0
20
00
04
08
12
16
20
LOCAL TIME (HOURS)

Fig. 4

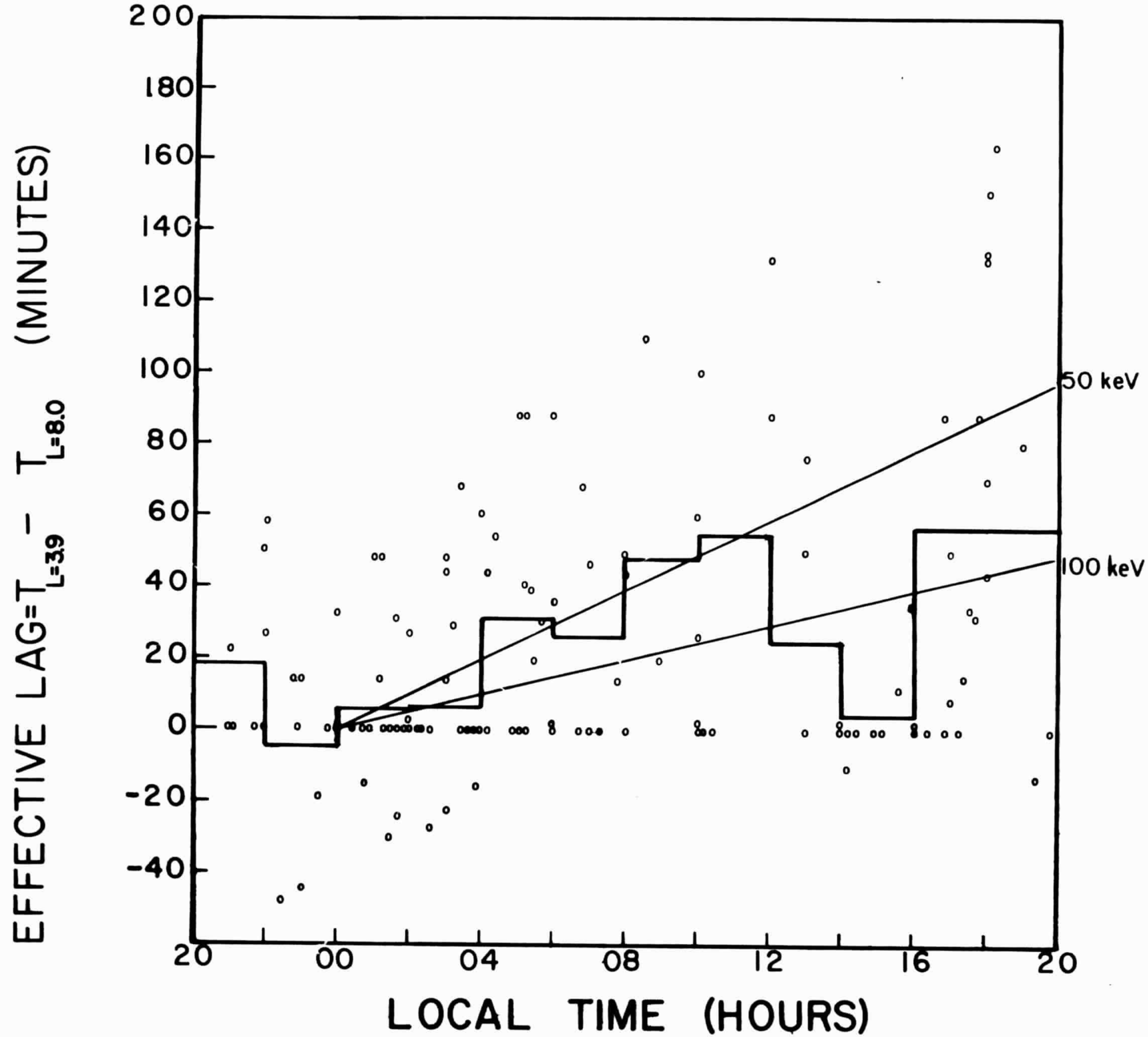
EFFECTIVE LAG=T L=3.9 − T L=8.0 (MINUTES)
200
180
160
140
120
100
80
60
40
20
0
-20
-40
20
00
04
08
12
16
20
LOCAL TIME (HOURS)
50 keV
100 keV

Fig. 5

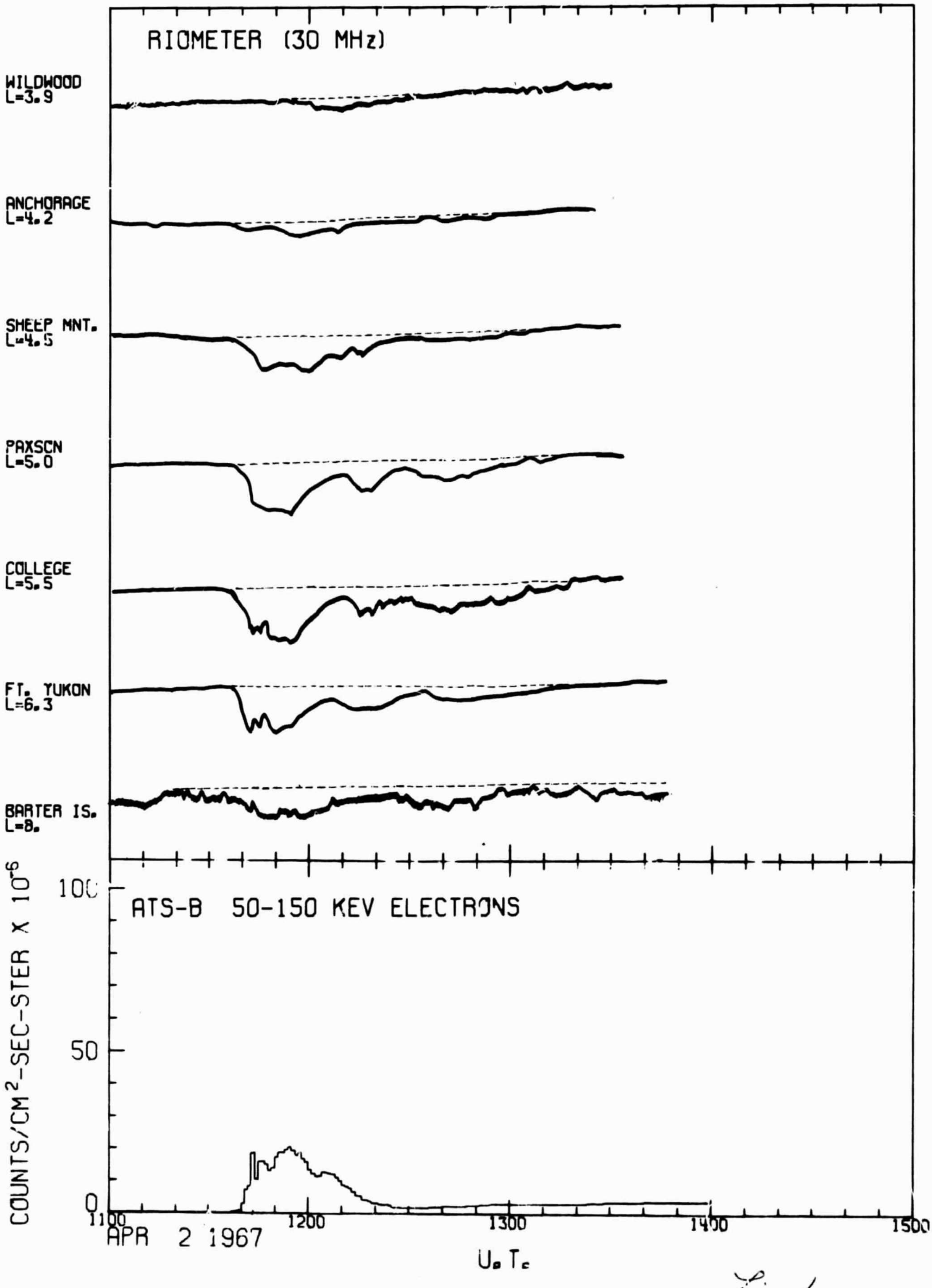
RIOMETER (30 MHz)
WILDWOOD L=3.9
ANCHORAGE L=4.2
SHEEP MNT. L=4.5
PAXSON L=5.0
COLLEGE L=5.5
FT. YUKON L=6.3
BARTER IS. L=8.
ATS-B 50-150 KEV ELECTRONS
COUNTS/CM²-SEC-STER X 10⁻⁶
100
50
0
1100
1200
1300
1400
1500
APR 2 1967
U. T.
Fig. 6

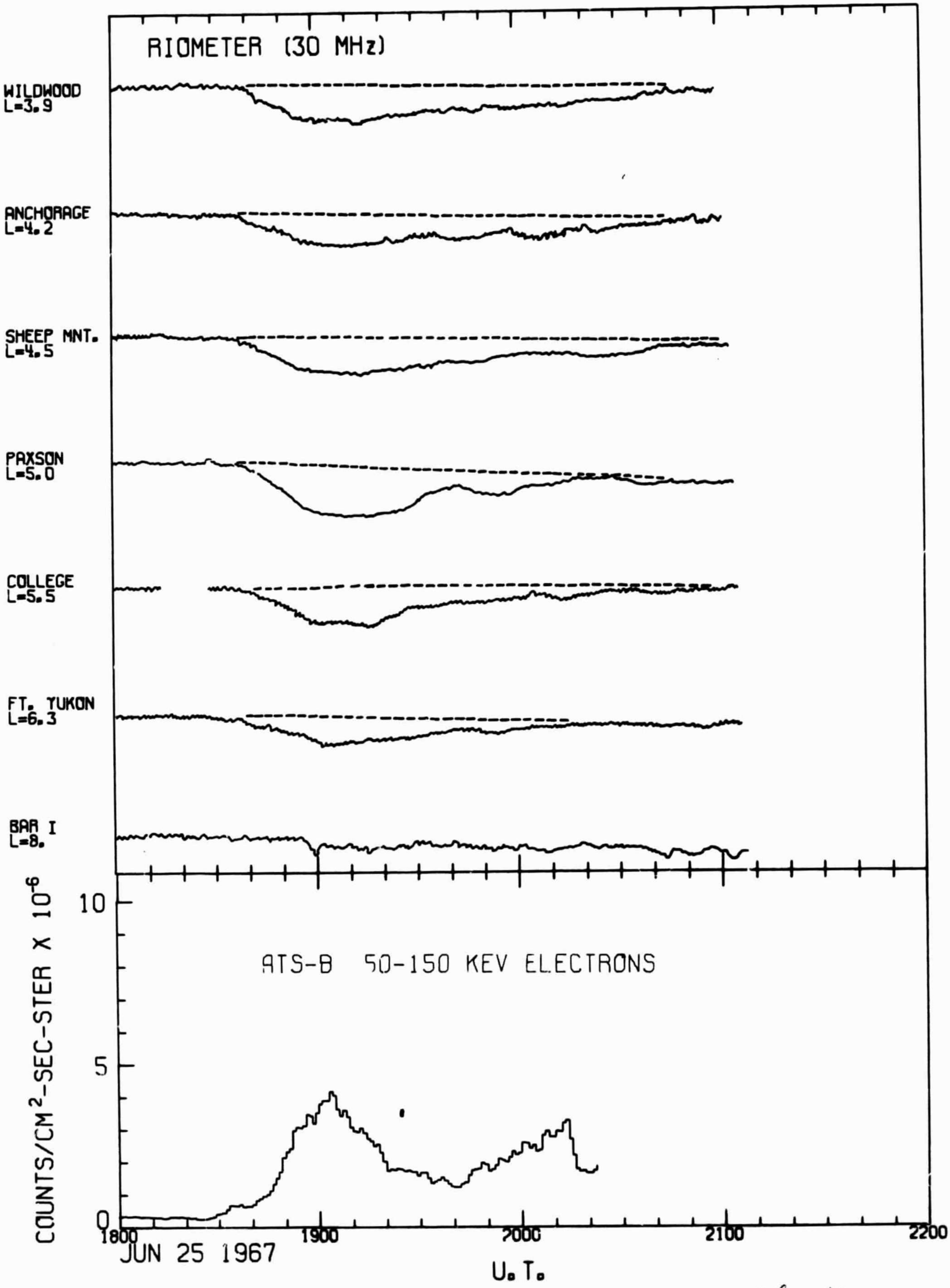

RIOMETER (30 MHz)
WILDWOOD L=3.9
ANCHORAGE L=4.2
SHEEP MNT. L=4.5
PAXSON L=5.0
COLLEGE L=5.5
FT. YUKON L=6.3
BAR I L=8.
ATS-B 50-150 KEV ELECTRONS
COUNTS/CM²-SEC-STER X 10⁻⁶
10
5
0
1800
1900
2000
2100
2200
JUN 25 1967
U. T.

Fig. 7

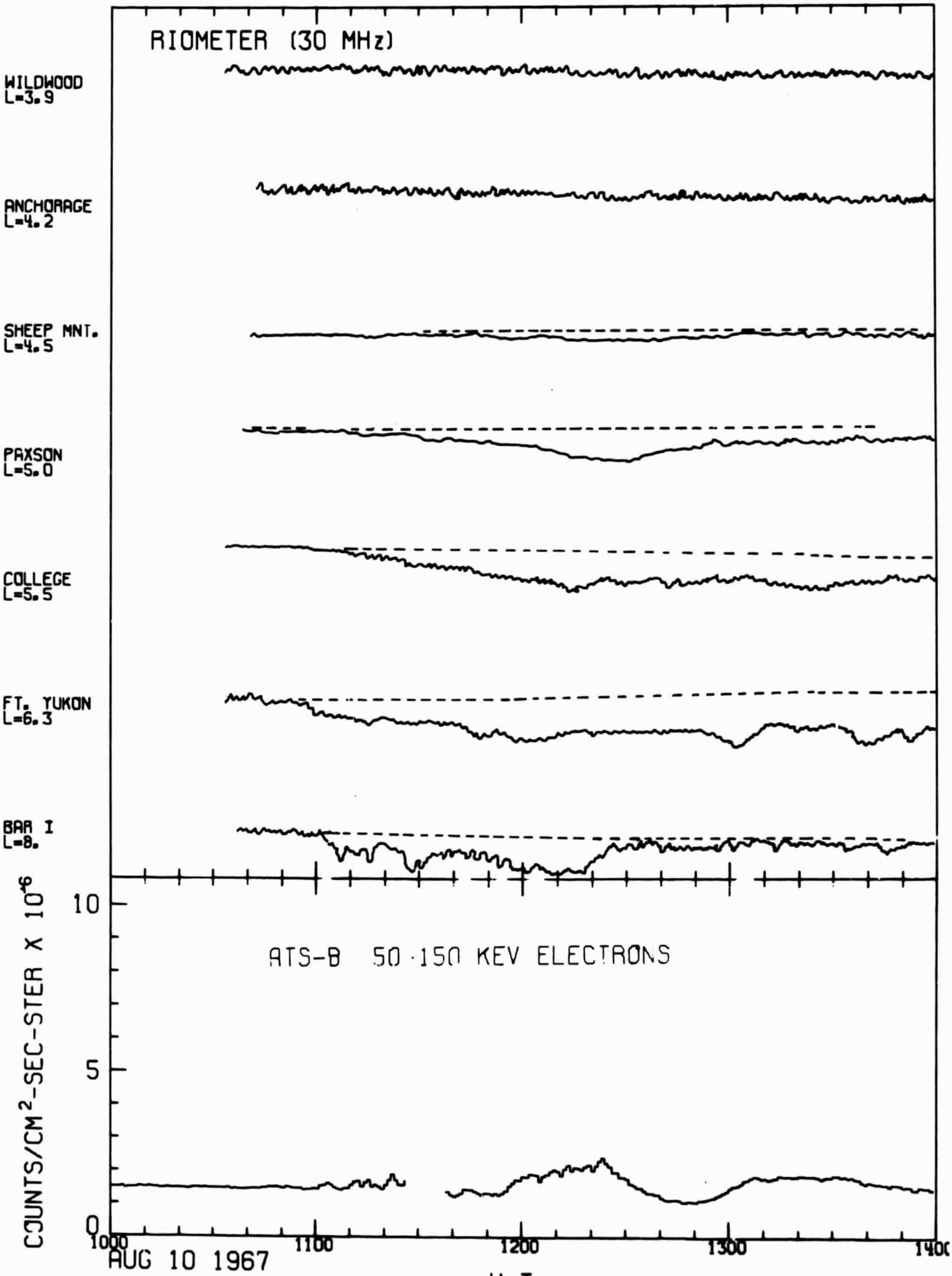
RIOMETER (30 MHz)
WILDWOOD L=3.9
ANCHORAGE L=4.2
SHEEP MNT. L=4.5
PAXSON L=5.0
COLLEGE L=5.5
FT. YUKON L=6.3
BAR I L=8.
ATS-B 50-150 KEV ELECTRONS
COUNTS/CM2-SEC-STER X 10-6
10
5
0
1000
1100
1200
1300
1400
AUG 10 1967
U. T.

Fig. 8

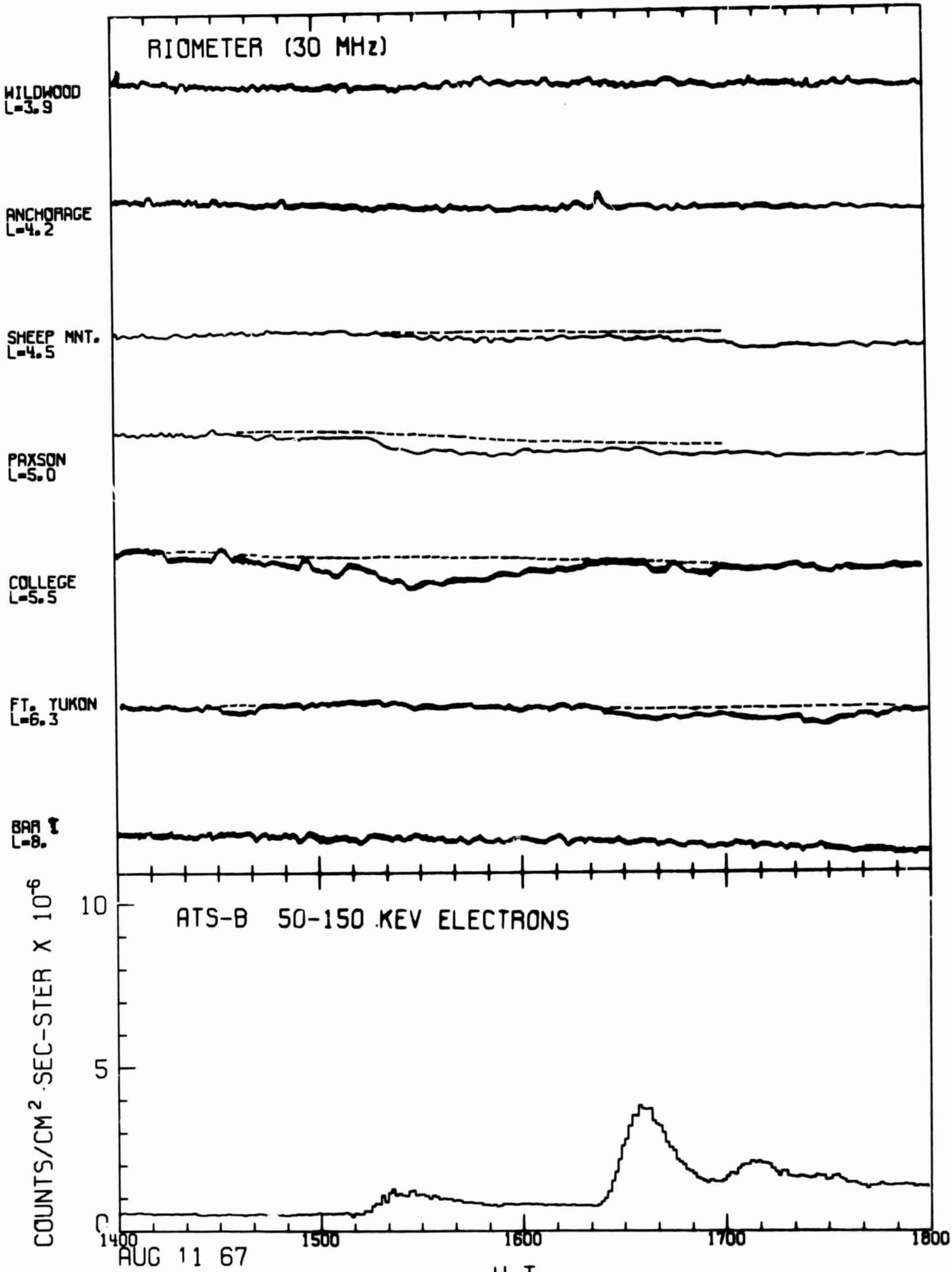
RIOMETER (30 MHz)
WILDWOOD L=3.9
ANCHORAGE L=4.2
SHEEP MNT. L=4.5
PAXSON L=5.0
COLLEGE L=5.5
FT. YUKON L=6.3
BAR I L=8.
ATS-B 50-150 KEV ELECTRONS
COUNTS/CM² SEC-STER X 10⁻⁶
10
5
0
1400
1500
1600
1700
1800
AUG 11 67
U. T.

Fig. 9

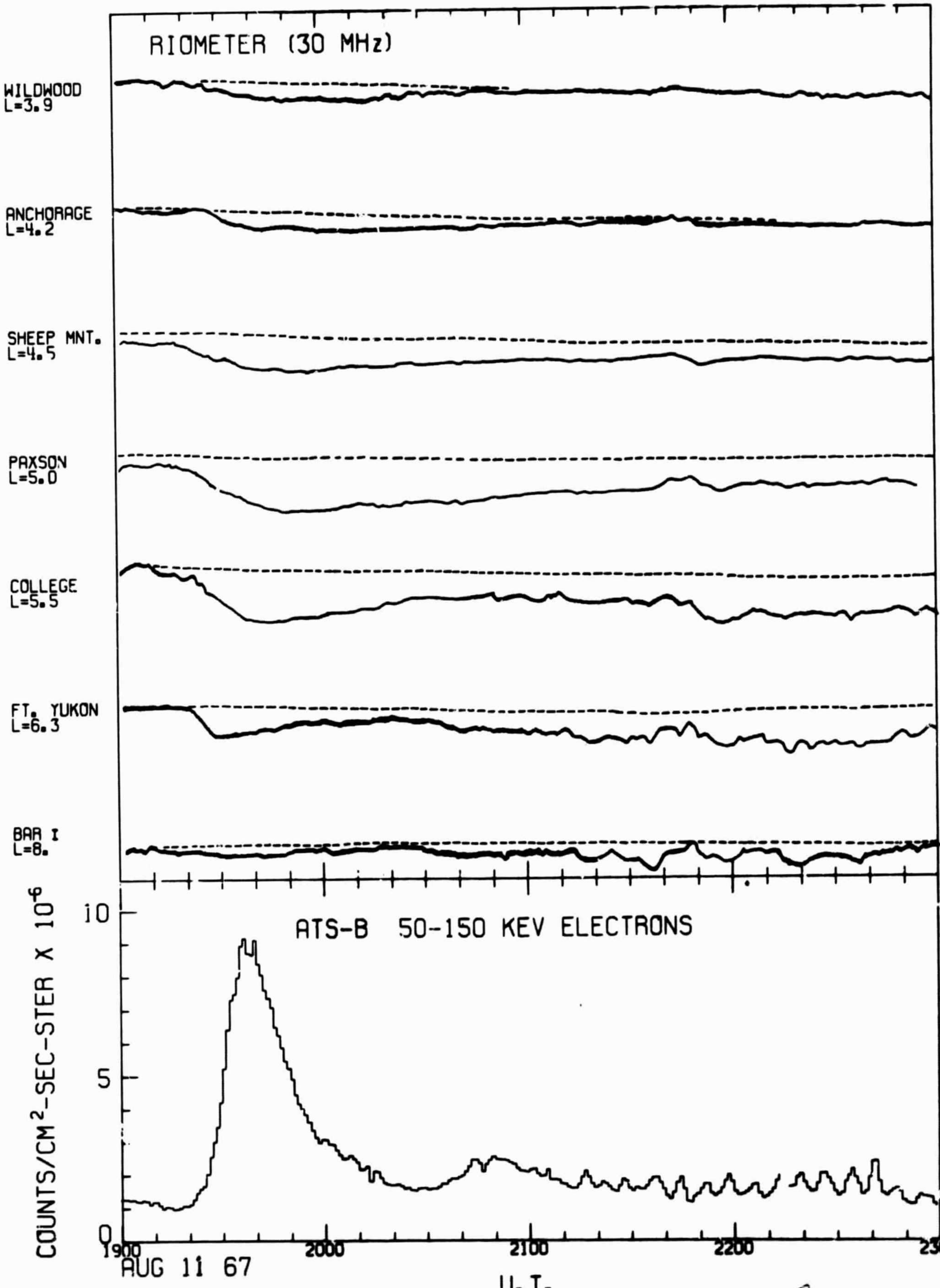
RIOMETER (30 MHz)
WILDWOOD L=3.9
ANCHORAGE L=4.2
SHEEP MNT. L=4.5
PAXSON L=5.0
COLLEGE L=5.5
FT. YUKON L=6.3
BAR I L=8.
ATS-B 50-150 KEV ELECTRONS
COUNTS/CM²-SEC-STER X 10⁻⁶
10
5
0
1900
2000
2100
2200
2300
AUG 11 67
U. T.

Fig. 10

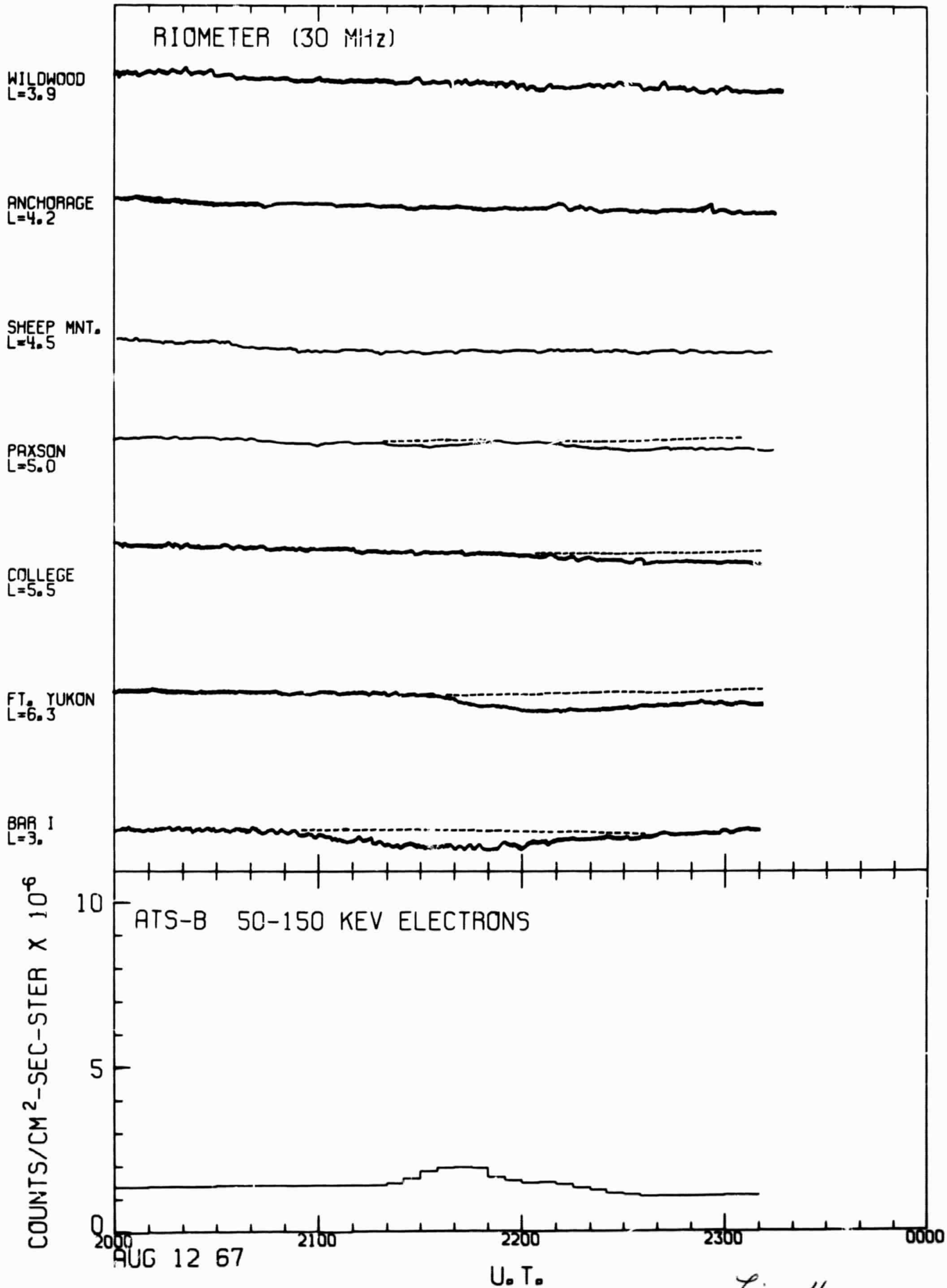
RIOMETER (30 MHz)
WILDWOOD L=3.9
ANCHORAGE L=4.2
SHEEP MNT. L=4.5
PAXSON L=5.0
COLLEGE L=5.5
FT. YUKON L=6.3
BAR I L=3.
ATS-B 50-150 KEV ELECTRONS
COUNTS/CM^2-SEC-STER X 10^6
10
5
0
2000
2100
2200
2300
0000
AUG 12 67
U. T.

Fig. 11

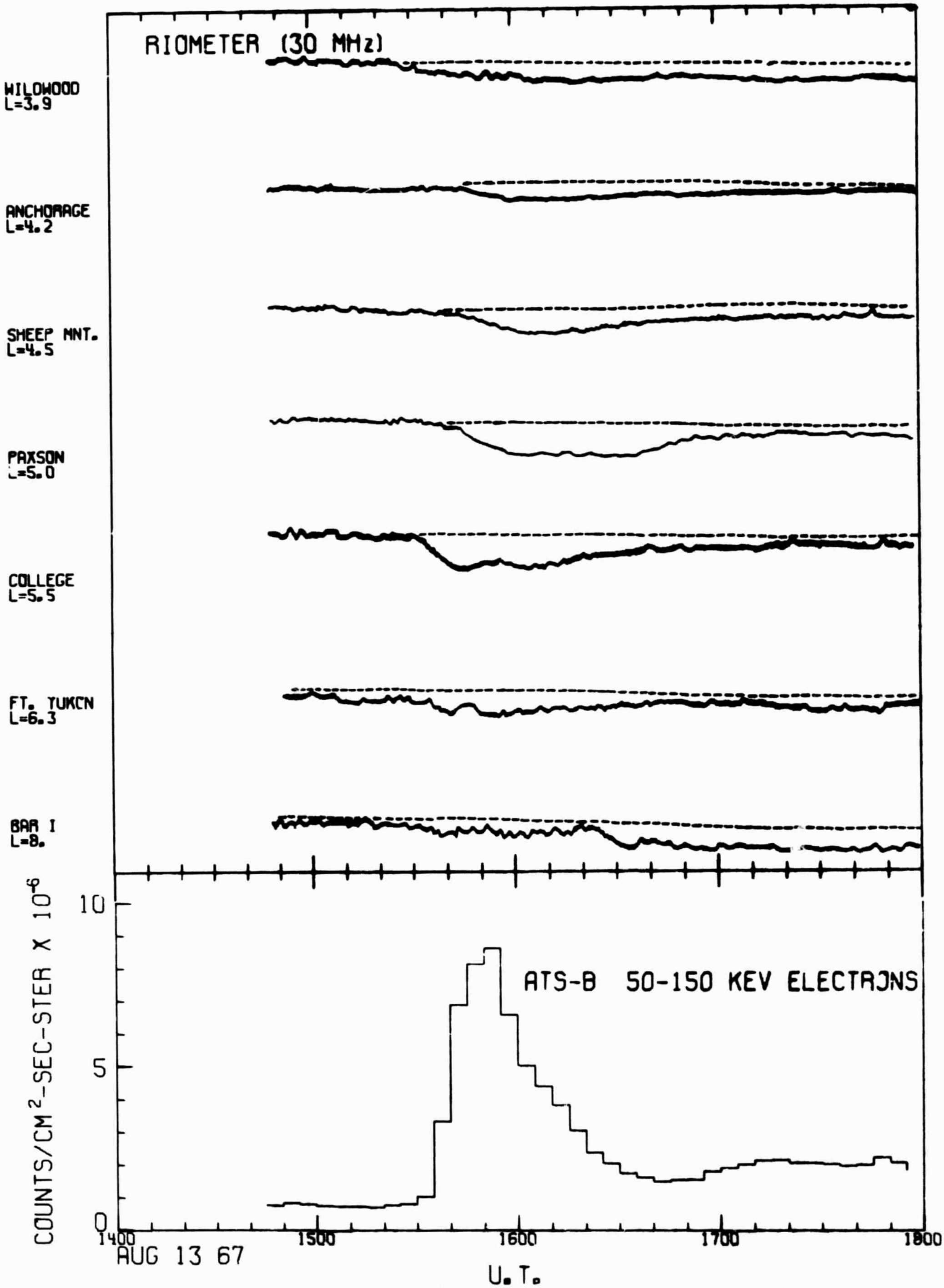

RIOMETER (30 MHz)
WILDWOOD L=3.9
ANCHORAGE L=4.2
SHEEP MNT. L=4.5
PAXSON L=5.0
COLLEGE L=5.5
FT. YUKON L=6.3
BAR I L=8.
COUNTS/CM²-SEC-STER X 10⁻⁶
10
5
0
ATS-B 50-150 KEV ELECTRONS
1400
1500
1600
1700
1800
AUG 13 67
U.T.

Fig. 12

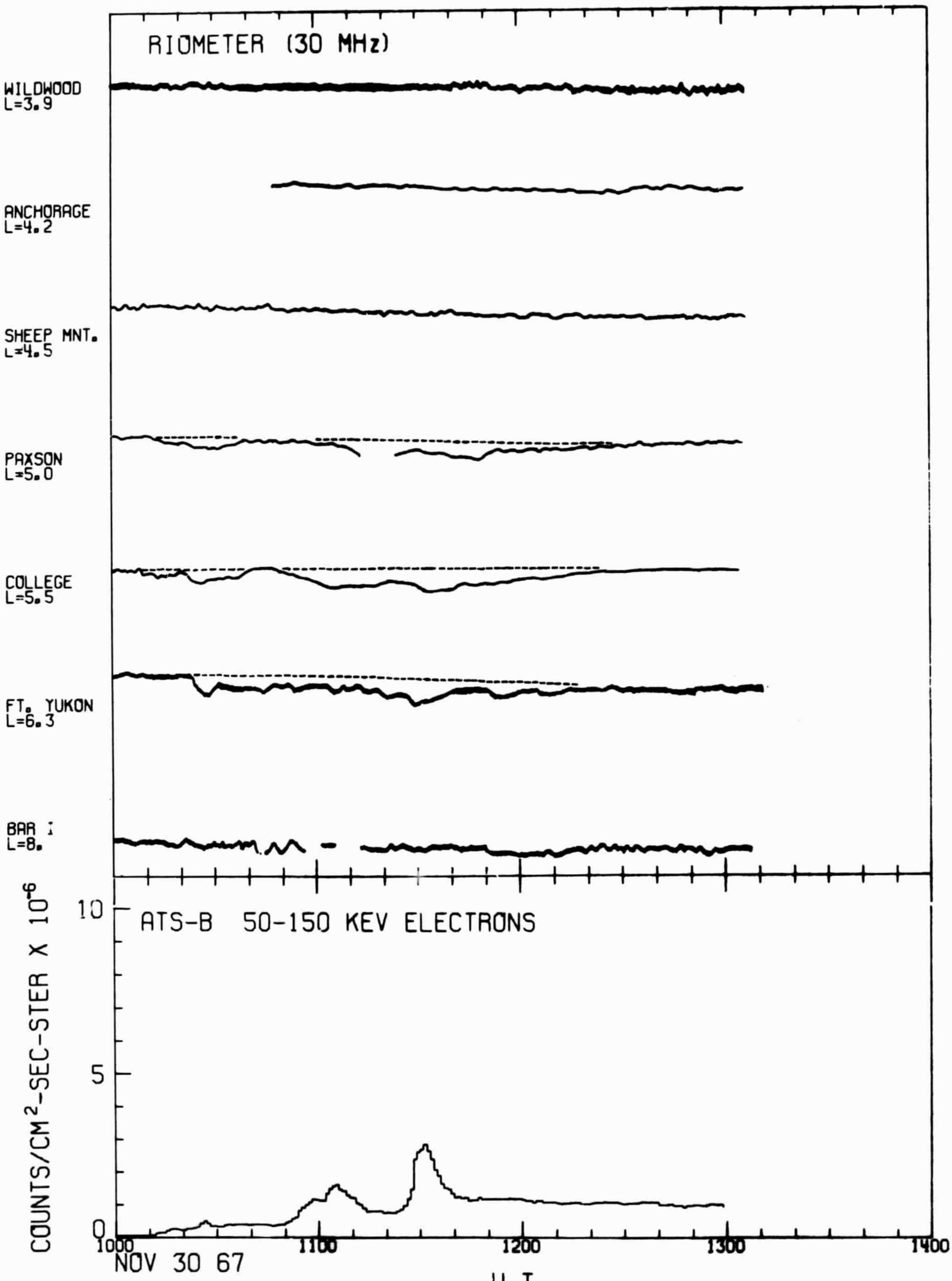
RIOMETER (30 MHz)
WILDWOOD L=3.9
ANCHORAGE L=4.2
SHEEP MNT. L=4.5
PAXSON L=5.0
COLLEGE L=5.5
FT. YUKON L=6.3
BAR I L=8.
ATS-B 50-150 KEV ELECTRONS
COUNTS/CM²-SEC-STER X 10⁻⁶
10
5
0
1000
1100
1200
1300
1400
NOV 30 67
U. T.

Fig. 13

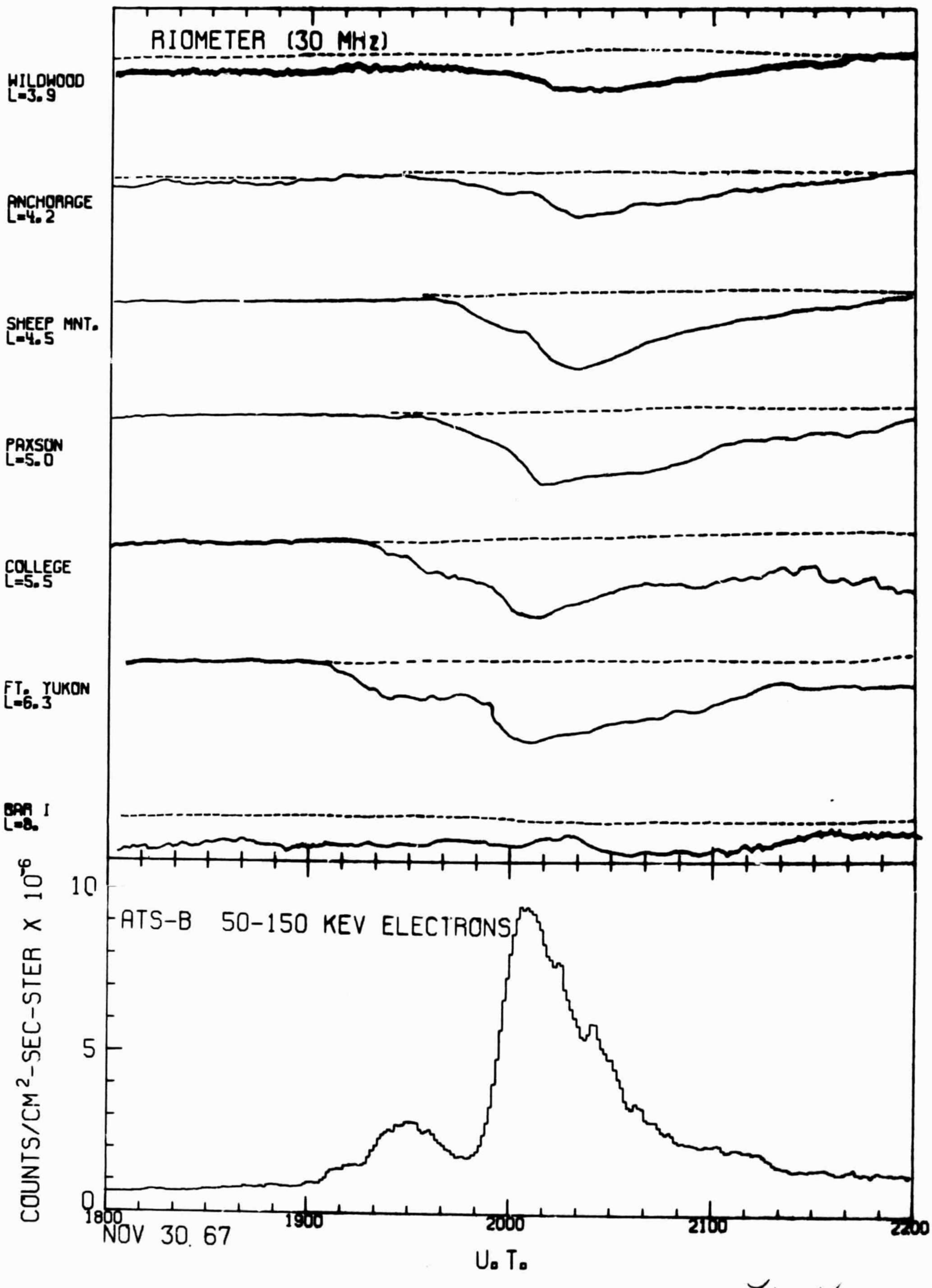
RIOMETER (30 MHz)
WILDWOOD L=3.9
ANCHORAGE L=4.2
SHEEP MNT. L=4.5
PAXSON L=5.0
COLLEGE L=5.5
FT. YUKON L=6.3
BAR I L=8.
COUNTS/CM^2-SEC-STER X 10^{-6}
10
5
0
ATS-B 50-150 KEV ELECTRONS
1800
1900
2000
2100
2200
NOV 30, 67
U. T.

Fig. 14

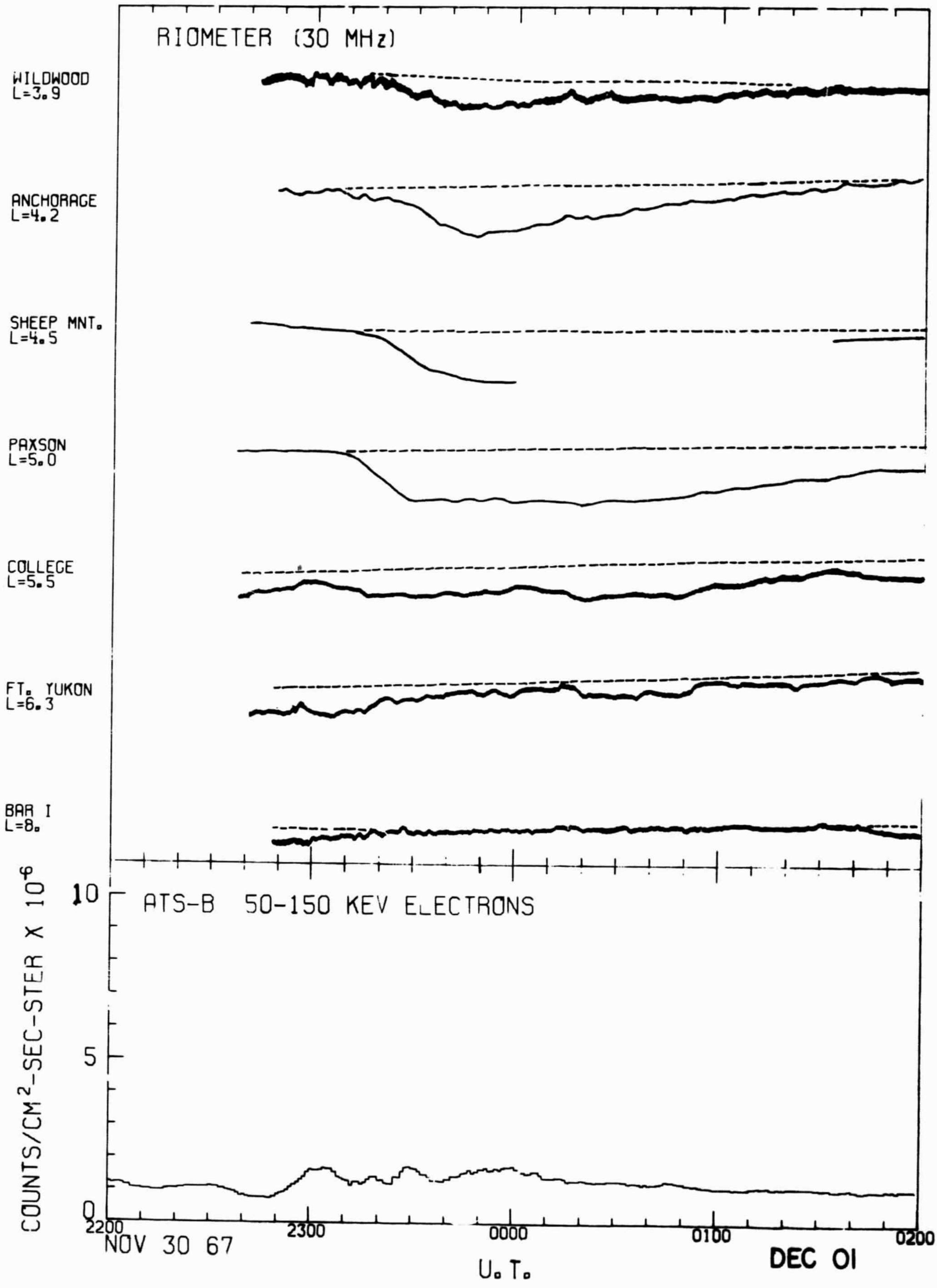

RIOMETER (30 MHz)
WILDWOOD L=3.9
ANCHORAGE L=4.2
SHEEP MNT. L=4.5
PAXSON L=5.0
COLLEGE L=5.5
FT. YUKON L=6.3
BAR I L=8.
ATS-B 50-150 KEV ELECTRONS
COUNTS/CM2-SEC-STER X 10^6
10
5
0
2200
2300
0000
0100
0200
NOV 30 67
U.T.
DEC 01

Fig. 15

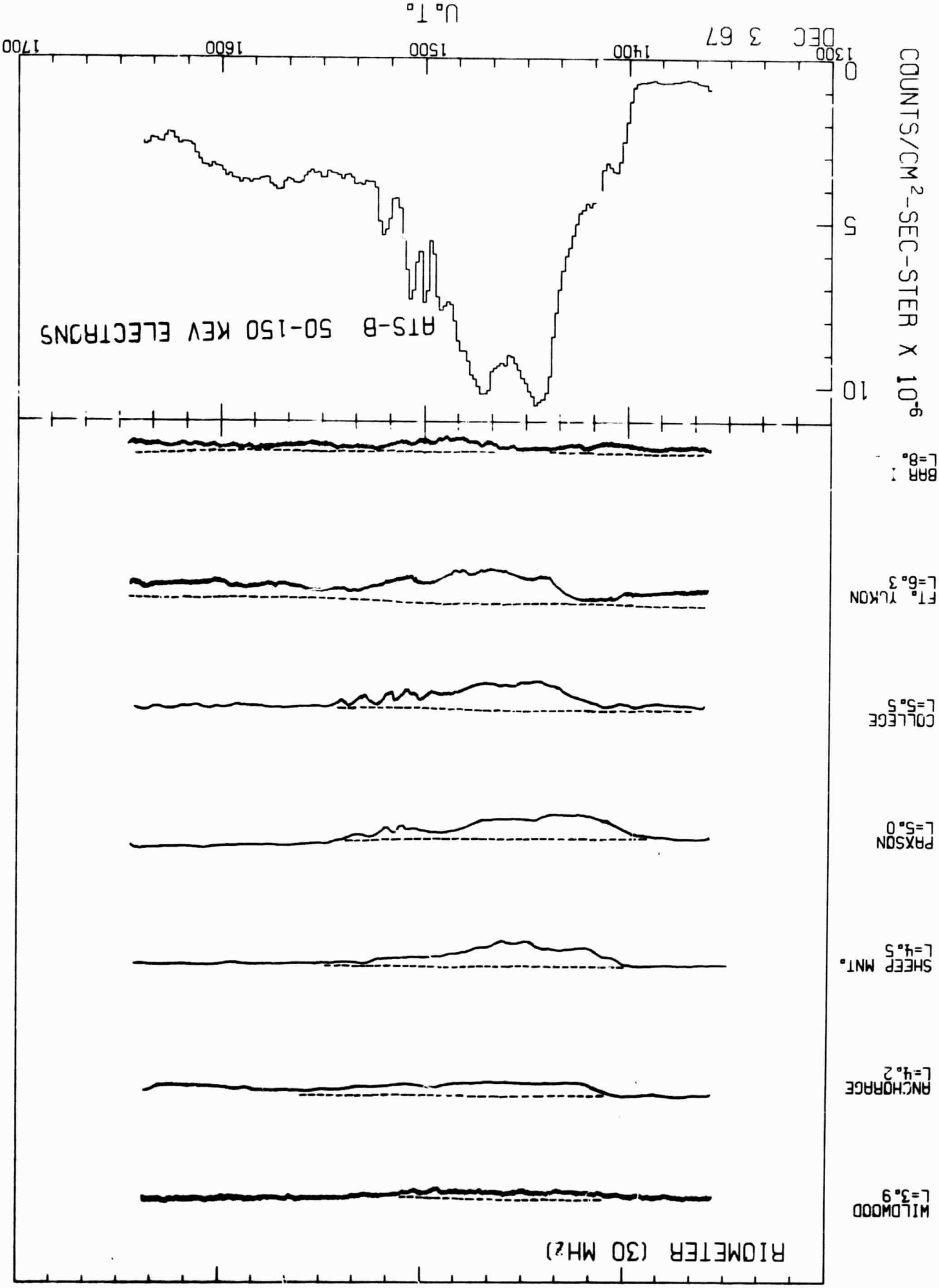

COUNTS/CM²-SEC-STER X 10⁻⁶
0
5
10
DEC 3 67
1300
1400
1500
1600
1700
U. T.
ATS-B 50-150 KEV ELECTRONS
BAR I L=8.
FT. YUKON L=6.3
COLLEGE L=5.5
PAXSON L=5.0
SHEEP MNT. L=4.5
ANCHORAGE L=4.2
WILDWOOD L=3.9
RIOMETER (30 MHz)

Fig. 16

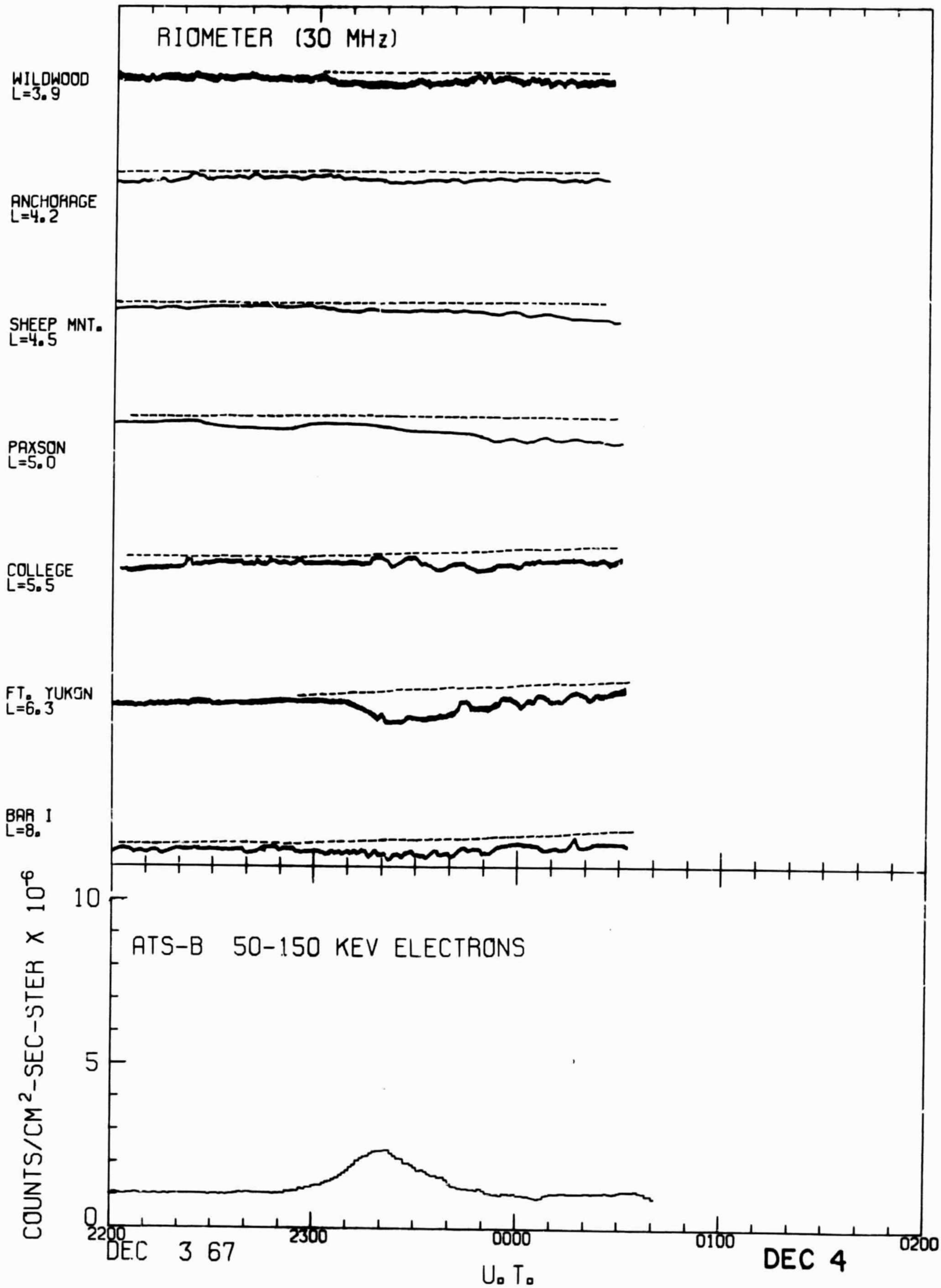
RIOMETER (30 MHz)
WILDWOOD L=3.9
ANCHORAGE L=4.2
SHEEP MNT. L=4.5
PAXSON L=5.0
COLLEGE L=5.5
FT. YUKON L=6.3
BAR I L=8.
ATS-B 50-150 KEV ELECTRONS
COUNTS/CM^2-SEC-STER X 10^6
10
5
0
2200
2300
0000
0100
0200
DEC 3 67
DEC 4
U. T.

Fig. 17

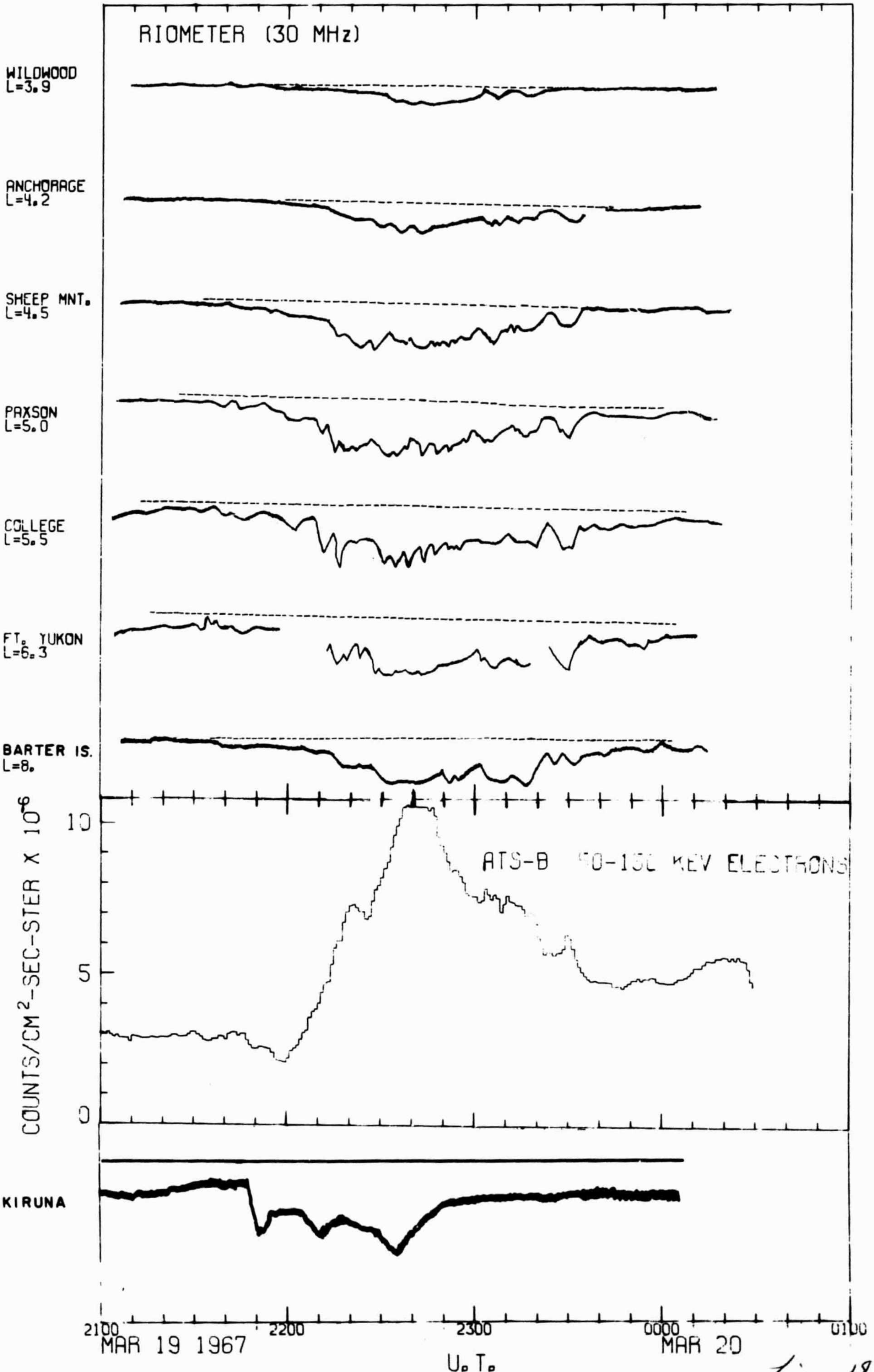

RIOMETER (30 MHz)
WILDWOOD L=3.9
ANCHORAGE L=4.2
SHEEP MNT. L=4.5
PAXSON L=5.0
COLLEGE L=5.5
FT. YUKON L=6.3
BARTER IS. L=8.
COUNTS/CM^2-SEC-STER X 10^6
10
5
0
ATS-B
KIRUNA
2100
2200
2300
0000
0100
MAR 19 1967
MAR 20
U. T.

Fig. 18

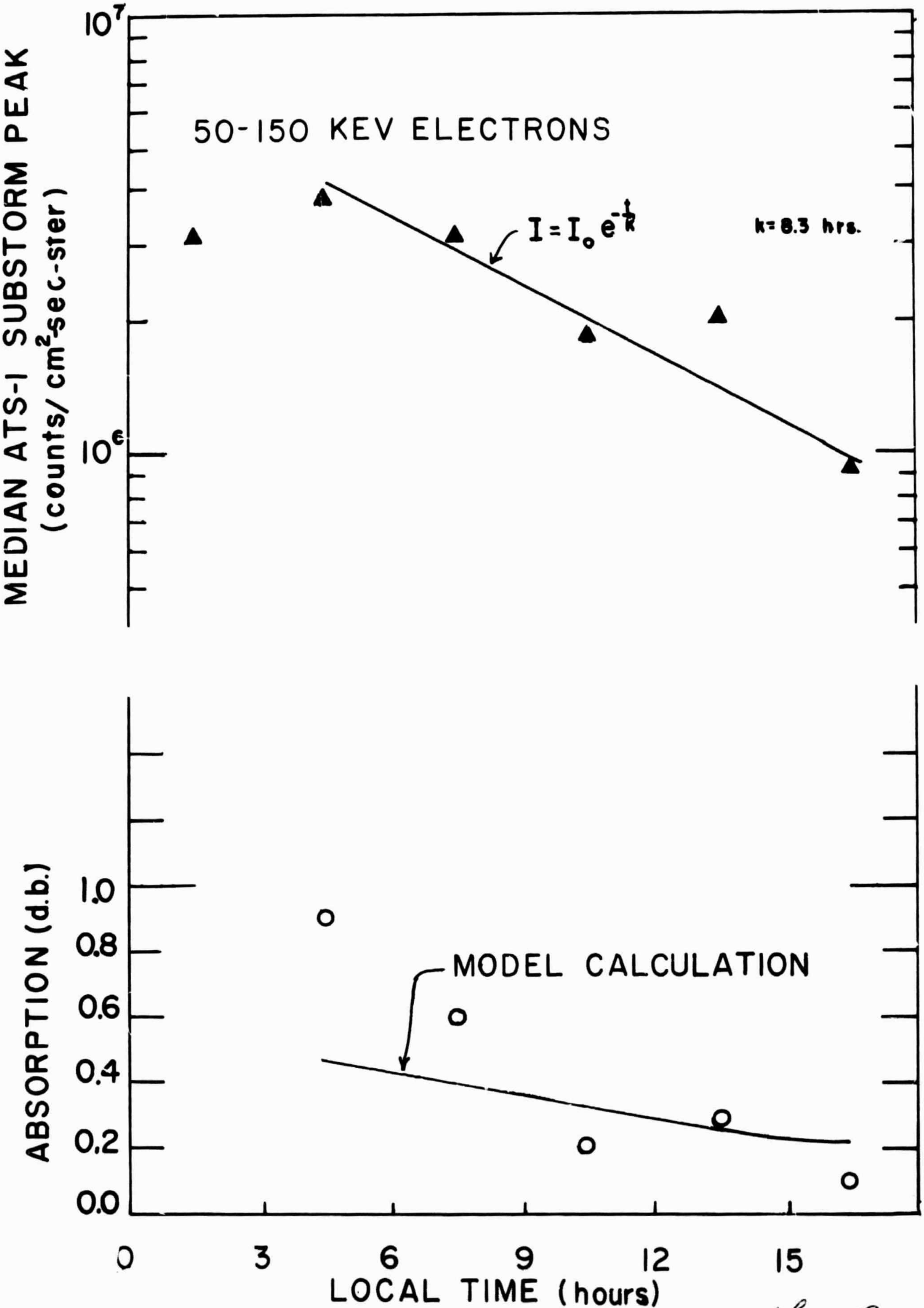

MEDIAN ATS-1 SUBSTORM PEAK (counts/cm²-sec-ster)
50-150 KEV ELECTRONS
$I = I_0 e^{-\frac{t}{k}}$
k=8.3 hrs.
ABSORPTION (d.b.)
MODEL CALCULATION
LOCAL TIME (hours)

Fig. 19

References

Akasofu, S. I., The Development of the Auroral Substorm, Planetary Space Sci., 12, 273, 1964.

Ansari, Z. A., The Aurorally Associated Absorption of Cosmic Noise at College, Alaska, J. Geophys. Res., 69, 4493, 1964.

Hargreaves, J. K., Auroral Motions Observed with Riometers: Movement Between Stations Widely Separated in Longitude, J. Atmospheric Terrest. Phys., 29, 1159, 1967.

Hartz, T. R. and N. M. Brice, The General Pattern of Auroral Particle Precipitation, Planetary Space Sci., 15, 301, 1967.

Jelly, D. and N. Brice, Changes in Van Allen Radiation Associated with Polar Substorms, J. Geophys. Res. 72, 5919, 1967.

Lezniak, T. W., R. L. Arnoldy, G. K. Parks and J. R. Winckler, Measurement and Intensity of Energetic Electrons at the Equator at 6.6 R_e, Radio Science, July, 1968, and University of Minnesota Technical Report CR-103.

Little, C. G. and H. Leinbach, Some Measurements of High-Latitude Ionospheric Absorption Using Extraterrestrial Radio Waves, Proc. IRE, 46, 334, 1958.

Parks, G. K., R. L. Arnoldy, T. W. Lezniak and J. R. Winckler, Correlation of Energetic Electrons between the Equator at 6.6 R_e and the Auroral Zone during Magnetospheric Substorms, Radio Science, July, 1968a and University of Minnesota Technical Report CR-103.

Parks, G. K., F. V. Coroniti, R. L. McPherron and K. A. Anderson, Studies of Magnetospheric Substorms, 1, Characteristics of Modulated Energetic Electron Precipitation Occurring during Auroral Substorms, J. Geophys. Res. 73, 1685, 1968b.

Parks, G. K. and J. R. Winckler, Acceleration of Energetic Electrons Observed at the Synchronous Altitude during Magnetospheric Substorms, J. Geophys. Res. 73, 5786, 1968.

Vasylunias, V. M., Low Energy Electrons on the Day Side of the Magnetosphere, J. Geophys. Res. 73, 7519, 1968.